Mineralium Deposita (2023) 58:379–402
https://doi.org/10.1007/s00126-022-01132-0

ARTICLE

Geology of the Altamira and Las Luces deposits, Coastal Cordillera, northern Chile: implications for the origin of stratabound Cu–(Ag) deposits

Ignacio Maureira[1,2] · Fernando Barra[1,2] · Martin Reich[1,2] · Gisella Palma[2,3]

Received: 7 January 2022 / Accepted: 11 July 2022 / Published online: 8 August 2022

Abstract

Stratabound Cu–(Ag) deposits in the Coastal Cordillera of northern Chile were emplaced under an extensional setting during the Late Jurassic and Early Cretaceous. Las Luces and Altamira are two stratabound Cu–(Ag) deposits located approximately at the same latitude (~25°45′S), but the former is hosted by Jurassic volcanic and volcaniclastic rocks, and the latter by Cretaceous volcano-sedimentary sequences. Both deposits show similar hydrothermal alteration types with albitization and hematite–chlorite superimposed on low-grade regional metamorphism. Sulfide mineralization is represented mainly by pyrite, chalcopyrite, and a bornite– "chalcocite" assemblage. Chalcopyrite is relatively minor and can replace early pyrite. In addition, framboidal pyrite of possible diagenetic origin was observed in Altamira. Copper mineralization is dominated by a bornite– "chalcocite" assemblage; however, electron probe analyses show that "chalcocite" has a composition ranging from geerite to djurleite. The typical mymekitic-like exsolution texture observed in the bornite–Cu sulfides assemblage is interpreted as caused by sub-solidus re-equilibration on cooling of the bornite–digenite solid solution. Silver, the main by-product in these deposits, is probably incorporated in solid solution in Cu sulfides and bornite, although Ag–sulfide microparticles were occasionally observed within sulfides in Altamira. Copper sulfides of the geerite–djurleite series can contain high amounts of Ag, ranging between 202 and 789 ppm, whereas in bornite from Las Luces Ag can reach up to 270 ppm. The presence of low-temperature (~ 100 °C) hydrothermal Cu sulfides is consistent with formation temperatures of < 300 °C, based on previous fluid inclusion studies. Bulk stable isotope data shows that sulfur in these deposits have different sources. In Las Luces $\delta^{34}S$ values for bornite and pyrite (− 2.5 to + 2.9‰) indicate a magmatic source, whereas in Altamira the negative values for "chalcocite" ($\delta^{34}S$: − 38.7 to − 10.7‰) are interpreted as sulfur derived by bacterial reduction of marine sulfate. The Las Luces and Altamira deposits were possibly formed by high water/rock ratios where basin-derived fluids leached metals from the volcanic/volcano-sedimentary host rocks. However, extensive leaching of the volcanic host rocks necessary to extract the Cu contained in silicate minerals is not consistent with the relatively small volume of hydrothermal alteration associated with these deposits, suggesting an additional magmatic contribution. In the revised genetic model, variable contributions of a magmatic and non-magmatic source are needed to form these stratabound Cu–(Ag) deposits.

Keywords Stratabound Cu–(Ag) deposits · Cu–(Fe) sulfides · Silver · Sulfur stable isotopes · Ore models · Northern Chile

Editorial handling: B. Lehmann

✉ Fernando Barra
fbarrapantoja@ing.uchile.cl

[1] Department of Geology and Andean Geothermal Center of Excellence (CEGA), FCFM, Universidad de Chile, Plaza Ercilla 803, Santiago, Chile

[2] Millennium Nucleus for Metal Tracing Along Subduction, FCFM, Universidad de Chile, Santiago, Chile

[3] Escuela de Geología, Universidad Mayor, Manuel Montt 367, Providencia, Santiago, Chile

Introduction

Stratabound Cu–(Ag) or "Chilean manto-type" deposits represent, after porphyry copper and iron-oxide copper–gold (IOCG) deposits, the third most important source of copper in Chile. These deposits occur in two metallogenic belts of different ages along the Coastal Cordillera of northern and central Chile (Fig. 1). The northern belt (18–26°S) comprises deposits hosted by volcanic to volcaniclastic sequences of Jurassic age (Kojima et al. 2009 and references therein). On the other hand, deposits from the north-central

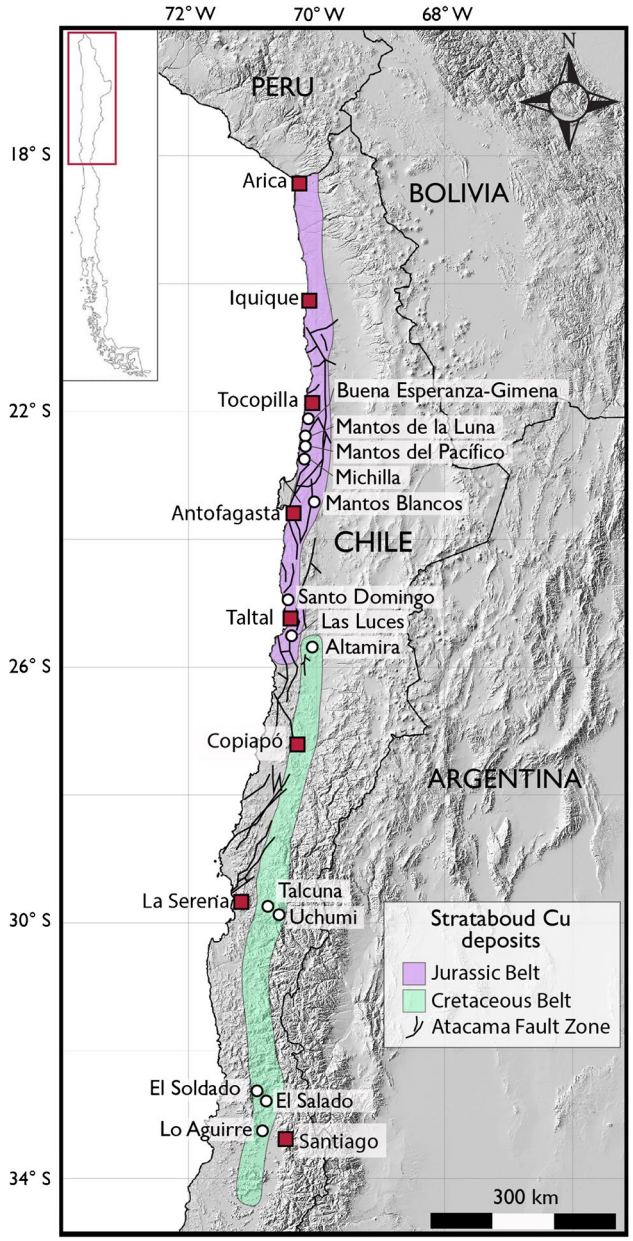

Fig. 1 Spatial distribution of the main stratabound Cu–(Ag) deposits in northern and central Chile. Trace of the AFZ taken from Brown et al. (1993)

Chile belt (26–34°S) formed within an intra-arc tectonic setting and are hosted by volcanic to volcano-sedimentary sequences of Early Cretaceous age (Zentilli et al. 1997; Boric et al. 2002; Cisternas and Hermosilla 2006) (Table 1).

The northern belt (18–26°S) comprises several deposits, among them Buena Esperanza, Mantos de la Luna, Mantos del Pacífico, Susana and Lince (Michilla district), Mantos Blancos, Santo Domingo, and Las Luces (Fig. 1; Table 1). These deposits are hosted mainly by basaltic to andesitic porphyritic lavas of the La Negra Formation (Rogers and Hawkesworth 1989; Oliveros et al. 2006, 2007), except for Mantos Blancos—the largest deposit in this belt—which is hosted by a bimodal suite of rhyolitic and andesitic rocks (Sato 1984; Maksaev and Zentilli 2002; Ramírez et al. 2006; Kojima et al. 2009). The porphyritic volcanic host rocks are composed of plagioclase, clinopyroxene with secondary minerals such as chlorite, epidote, quartz, sericite, calcite, hematite, and minor amounts of zeolites, prehnite, pumpellyite, and actinolite. The formation of these secondary minerals has been attributed to both burial metamorphism (i.e., zeolite to greenschist facies) and hydrothermal alteration caused by the emplacement of the Coastal Batholith (Losert 1974; Sato 1984; Oliveros et al. 2005, 2008). The La Negra Formation was intruded by Jurassic to Early Cretaceous plutons of gabbroic to granodioritic composition (Kojima et al. 2003; Wilson et al. 2003a), and andesitic subvolcanic intrusive bodies, such as dikes, sills, stocks, or volcanic necks (Maksaev and Zentilli 2002). Published K–Ar and $^{40}Ar/^{39}Ar$ dates indicate that the emplacement of the plutonic bodies occurred mainly between 168 and 147 Ma (Ulriksen 1979; Boric et al. 1990; Maksaev 1990; Maksaev and Zentilli 2002), whereas ages obtained from the subvolcanic bodies and alteration phases related to the mineralization range between 168 and 100 Ma (Boric et al. 1990; Wilson et al. 2003a; Oliveros et al. 2006).

In the northern belt, Cu mineralization occurs disseminated and in amygdale fillings, stockworks, veins, and breccias (Kojima et al. 2009). The general paragenetic sequence is characterized by an early stage with pyrite–chalcopyrite followed by the precipitation of hypogene Cu sulfides (chalcocite–digenite), bornite, and specular hematite. The hydrothermal alteration that affected the volcanic host rocks is dominated by Na metasomatism represented by selective albitization of primary plagioclase, followed by calcic alteration with epidote, chlorite, calcite, and minor actinolite, sericite, quartz (Elgueta et al. 1990; Kojima et al. 2003; Cisternas and Hermosilla 2006).

Stratabound Cu–(Ag) deposits from the central belt (26–34°S) formed within intra-arc basins that comprise Lower Cretaceous volcanic to volcano-sedimentary sequences, including sandstones, tuffaceous siltstones, and limestones (Camus 1990; Sillitoe 2003; Maksaev and Zentilli 2002; Kojima et al. 2009). The largest deposits of this belt are El Soldado and Lo Aguirre, both hosted in volcanic rocks, whereas deposits from the Talcuna and Arqueros districts are hosted mainly in volcaniclastic sequences (Oyarzún et al. 1998; Wilson et al. 2003a, b; Table 1). Hypogene mineralization is represented by pyrite, chalcopyrite, bornite, chalcocite, minor galena, and sphalerite. Common gangue minerals are chlorite, calcite, epidote, hematite, and locally magnetite. Zeolites, pumpellyite, and prehnite are usually found filling vesicles in the volcanic rocks, evidencing regional low-grade metamorphism

Table 1 Main geologic characteristics of the most important stratabound Cu(–Ag) deposits in northern and central Chile

Deposit	Host Rock	Mineralization	Alteration	Geochronology		Tonnage	Reference
				Alteration	Mineralization		
Jurassic belt							
Mantos Blancos	Rhyolite–andesite (La Negra Fm)	Ccp–Bn–Dg–Gn	Qz–Ser; Kfs; Chl–Ab	155–141 Ma ($^{40}Ar/^{39}Ar$)		500 Mt at 1% Cu	Ramírez et al. (2006)
Michilla district	Andesite (La Negra Fm)	Cct–Bn–Ccp; Atm–Ccl	Chl–Ep–Ab		~160 Ma (Re–Os)	16 Mt at 1.56% Cu	Boric et al. (1990); Tristá-Aguilera et al. (2006)
Buena Esperanza	Basalt–andesite (La Negra Fm)	Cct–Bn–Ccp–Dg	Ab–Chl–Qz–Kfs–Ser	~168 Ma (K–Ar)		7 Mt at 2.9% Cu	Boric et al. (1990)
Santo Domingo	Basalt–andesite (La Negra Fm)	Cct–Bn–Ccp	Ab–Chl–Cal–Qz–Hem–Ser	139–129 Ma (K/Ar)		2.3 Mt at 2.3% Cu	Boric et al. (1990)
Las Luces	Basalt–andesite (La Negra Fm)	Cct–Dg–Bn–Ccp–Gn	Ab–Chl–Qz–Ser–Cal			2.3 Mt at 1.11% Cu	Zamora (2011a)
Mantos de La Luna	Basalt–andesite (La Negra Fm)	Cct–Dg–Bn, Ccp	Cal–Qz–Hem			60 Kt/month at 1.7% Cu	Kojima et al. (2003)
Mantos del Pacífico	Andesite (La Negra Fm)	Ccp–Bn, Ccl	Cal–Qz–Hem				Vivallo and Henríquez (1998)
Cretaceous belt							
Altamira	Basalt–andesite (Aeropuerto Fm)	Cct–Dg–Bn–Ccp	Ab–Chl–Qz–Ser–Cal		~90 Ma (Re–Os cct)	2.86 Mt at 1.24% Cu, Ag 34 ppm	Zamora (2011b), Barra et al. (2017)
El Soldado	Basalt–rhyodacite (Lo Prado Fm)	Cct–Ccp–Bn	Bit, Ab–Kfs–Cal	103 Ma ($^{40}Ar/^{39}Ar$)		200 Mt at 1.35% Cu	Boric et al. (2002); Wilson et al. (2003a)
Lo Aguirre	Dacite, andesite, breccias (Veta Negra Fm)	Cct–Bn–Ccp ± Py–Hm	Ab–Ser–Qz	102 ± 5 Ma ($^{40}Ar/^{39}Ar$)		19 Mt at 1.66%	Saric et al. (2003)
Talcuna district	Volcanic and volcaniclastic rocks (Quebrada Marquesa Fm)	Sph, Ccp–Bn > Cct, Cv, Tnt–Ttr,	PyBit, Cal–Chl–Ser–Qz			15 Mt at 1% Cu	Oyarzún et al. (1998), Wilson and Zentilli (2006)

Table 1 (continued)

Deposit	Host Rock	Mineralization	Alteration	Geochronology	Tonnage	Reference
Ocoita-Pabellón district	Andesite–marine carbonates (Pabellón Fm)	Ccp, Bn > Cct, Cv, Tnt–Ttr	Bit, Cal–Qz–Chl–Zeo		30–130 tons/month at 3.0% Cu	Cisternas and Hermosilla (2006)
Arqueros district	Volcanic and volcaniclastic units (Arqueros Fm)	Arq–Arg–Ag°–PyAg–CeAg	Bar, Cal			Oyarzún et al. (1998)
Uchumi	Arkosic conglomerate	Bn–Cct, Cv	Qz–PyBit–Cal–Clays			Wilson and Zentilli (2006)
Cabildo district	Volcanic and sedimentary rocks (Lo Prado Fm)	Bn–Ccp, Sph, Gn	Cal, Chl–Prh–Ab			Moreno-Rodríguez et al (2010)

Abbreviations: *Ab*, albite; *Ag°*, native silver; *Arg*, argentite; *Arq*, arquerite; *Atm*, atacamite; *Bar*, baritine; *Bit*, bitumen; *Bn*, bornite; *Cal*, calcite; *Cct*, chalcocite; *Ccp*, chalcopyrite; *Ccl*, chrysocolla; *Chl*, chlorite; *Cv*, covellite; *Dg*, "chalcocite"; *Ep*, epidote; *Gn*, galena; *Hem*, hematite; *Kfs*, K-feldespar; *Prh*, prehnite; *PyBit*, pyrobitumen; *Qz*, quartz; *Ser*, sericite; *Sph*, Sphalerite; *Tnt–Ttr*, tennantite–tetrahedrite; *Zeo*, zeolite

(Zentilli et al. 1997; Wilson and Zentilli 1999; Morales et al. 2005; Kojima et al. 2009).

One distinct difference between the deposits hosted in Cretaceous and Jurassic rocks is the presence of residual (solid) petroleum or (pyro)bitumen associated with the Cu–(Ag) mineralization in Cretaceous deposits (Zentilli et al. 1997; Wilson et al. 2003b; Cisternas and Hermosilla 2006), although recently Herazo et al. (2020) reported the first occurrence of bitumen in the Lorena deposit in Jurassic rocks in the Las Luces district. Some studies show that (pyro)bitumen might play a fundamental role in the formation of these deposits acting as a redox trap for Cu-bearing hydrothermal fluids, triggering sulfide precipitation (Zentilli et al. 1997; Wilson and Zentilli 1999) and possibly as a source of sulfur (Herazo et al. 2020).

The timing of ore formation in stratabound Cu–(Ag) deposits has proven challenging due to the scarce presence of proper alteration mineral phases to be dated using traditional methods (K–Ar, $^{40}Ar/^{39}Ar$, U–Pb). Hence, the formation age of these deposits has been inferred mostly by dating the volcanic host rocks and intrusions. Oliveros et al. (2006) constrained the volcanic activity of La Negra Formation between ca. 170 to 150 Ma by using $^{40}Ar/^{39}Ar$ thermochronology, whereas the Cu mineralization in the Michilla district was circumscribed to a ~ 27 Ma period between 164 and 137 Ma (Oliveros et al. 2008). Similarly, in La Serena area (29°30′–30°00′S, Fig. 1), a lava flow from the Arqueros Formation was dated at 114.1 ± 0.5 Ma ($^{40}Ar/^{39}Ar$ on primary Ca-plagioclase; Morata et al. 2008), and a K–Ar age from celadonite associated with sulfides at the Talcuna mine yielded an age of 93 ± 2 Ma (Morata et al. 2006), supporting a Cretaceous age for the Cu mineralization. In the El Soldado deposit, the age of mineralization has been constraint at ca. 103 Ma by $^{40}Ar/^{39}Ar$ K-feldspar dating (Wilson et al. 2003a). Few attempts have been made to date the ore mineralization using Re–Os systematics. Tristá-Aguilera et al. (2006) reported a poorly constrained Re–Os isochron age of 160 ± 16 Ma (2σ, $n = 4$, MSWD = 1.8) obtained from the analyses of chalcocite and chalcocite ± bornite samples from the Lince-Estefania ore deposit, Michilla district (Fig. 1); an age that is broadly consistent with $^{40}Ar/^{39}Ar$ dates from the La Negra host rocks. More recently, Barra et al. (2017) reported a ~ 90 Ma Re–Os model age for Altamira, which supports a Cretaceous age for this deposit.

Although Chilean manto-type Cu–(Ag) deposits have been extensively studied, genetic models remain contentious. Early studies proposed a syngenetic model for their formation (e.g., Ruíz et al. 1965; Stoll 1965), although most authors support an epigenetic model based on the geometry of the ore bodies, the spatial relationship of the Cu mineralization around intrusive stocks and sills, and the presence of widespread hydrothermal alteration associated with Cu-rich sulfide disseminations (Maksaev

and Zentilli 2002). Two main ideas have developed around the epigenetic model: (a) a magmatic-hydrothermal origin where fluids and metals are derived from a magmatic source (e.g., Palacios 1990; Vivallo and Henríquez 1998; Maksaev and Zentilli 2002; Ramírez et al. 2006), and (b) Cu was leached from the volcanic host rocks by fluids of metamorphic or non-magmatic (basinal brines, connate, and meteoric waters) origin and where the intrusions provided heat for hydrothermal convection (Losert 1973; Sato 1984; Boric et al. 1990; Oyarzún et al. 1998; Tosdal and Munizaga 2003; Wilson et al. 2003a, b; Kojima et al. 2009). Limited Re–Os data on sulfides from stratabound Cu–(Ag) deposits in northern Chile (Lince-Estefania, Tristá-Aguilera et al. 2006; Altamira, Barra et al. 2017) show radiogenic initial Os ratios, suggesting a significant crustal component for the Os contained in the copper sulfides. In addition, sulfur isotope data for Jurassic deposits show a distinctive magmatic signature, whereas bitumen-bearing deposits are characterized by largely negative $\delta^{34}S$ values, indicating sulfur derived from bacterial and/or thermochemical reduction of sulfate (Wilson and Zentilli 1999; Wilson et al. 2003b; Carrillo-Rosúa et al. 2014).

Stratabound Cu deposits from north and central Chile contain relevant concentrations of Ag; however, little is known about its form of incorporation in Cu sulfides and their concentrations in Cu-bearing phases. Furthermore, the origin and composition of the Cu sulfides—broadly named as "chalcocite"—and their textures are poorly understood. The purpose of this study is to provide new insights on the origin of stratabound Cu–(Ag) deposits from northern Chile by studying the Altamira and Las Luces deposits; both located at about the same latitude (26°S; Fig. 1), but apparently formed at different times. These two deposits, despite being currently mined, have not been studied in detail. Their proximity and inferred formation age (Las Luces: Jurassic and Altamira: Cretaceous) present a unique opportunity to test the proposed epigenetic models for stratabound Cu–(Ag) deposits by comparing their geological, geochemical, and mineralogical characteristics. In addition, we investigate the composition of the Cu sulfides to determine their possible origin and evaluate the concentration and distribution of Ag in the main Cu ore minerals.

In this contribution, we present new petrographic and ore mineralogy descriptions of ore bodies and host rocks from Las Luces and Altamira in order to establish the mineralization and alteration events for each deposit. These data provides a general framework for the analytical studies, interpretations, and discussion. Electron probe microanalyses (EPMA) on selected ore sulfides were performed to quantify the presence of major (Cu, Fe, S) and minor elements of interest (i.e., Ag, As, Sb, Se, Te, Au, Ni, Co, and Hg). We also performed bulk sulfur isotope analyses of sulfide concentrates to determine the source of sulfur in certain sulfide phases (i.e., magmatic or bacteriogenic). We also evaluated the magmatic-hydrothermal contribution vs. host rock leaching hypotheses to better understand the formation of these deposits and provide a revised genetic model for stratabound Cu–(Ag) deposits in Chile.

Geological background

The oldest formation recognized in the study area is the Las Tórtolas Formation (Devonian-Carboniferous), which comprises quartzites, slates, phyllites, and mica schists that outcrop in the coastal area near Cifuncho (Fig. 2). This formation represents deposition of terrigenous sediments (interstratified sandstones and shales) with lesser limestones, cherts, and mafic volcanic rocks in a marine environment. This sequence was later affected by low-grade metamorphism and deformation (Naranjo and Puig 1984; Maksaev 1990; Boric et al. 1990).

The Triassic Cifuncho Plutonic Group comprises syenogranite and monzogranite stocks that intruded the Las Tórtolas Formation and is covered by sedimentary and volcanic rocks of the Cifuncho Formation (Fig. 2; Naranjo and Puig 1984). The latter is exposed in the current Coastal Cordillera and unconformably overlies the Las Tórtolas metasedimentary rocks and conformably underlies the Early Jurassic sedimentary rocks of the Pan de Azúcar Formation (Fig. 2; Maksaev 1990; Boric et al. 1990). These Early Jurassic rocks (Hettangian–Sinemurian) correspond to a stratified package of sandstones, fine-grained conglomerates, tuffs, calcareous sandstones, and shales (Naranjo and Puig 1984). The Late Triassic to Early Jurassic Tigrillo Plutonic Group (Fig. 2) intruded the metasedimentary rocks of the Las Tórtolas Formation and is overlain by Jurassic volcanic lavas of the La Negra Formation (Boric et al. 1990).

A subduction-related magmatic arc system was established along the Coastal Cordillera of northern Chile (Mpodozis and Ramos 1990; Maksaev and Zentilli 2002; Jara et al. 2021) during the Late Jurassic to Early Cretaceous. This magmatic activity resulted in a thick (> 7000 m) basaltic to andesitic volcanic sequence with minor sandstones, shales, and fossiliferous limestones emplaced over a thinned pre-Jurassic continental crust (Scheuber and González 1999; Maksaev and Zentilli 2002). The Jurassic stratabound Cu–(Ag) deposits are hosted mostly in this thick volcanic sequence known as La Negra Formation. This formation was later intruded by several mafic to felsic stocks and dikes of Early Jurassic to Lower Cretaceous age that range in composition from gabbro to diorite and granodiorite with scarce tonalite and

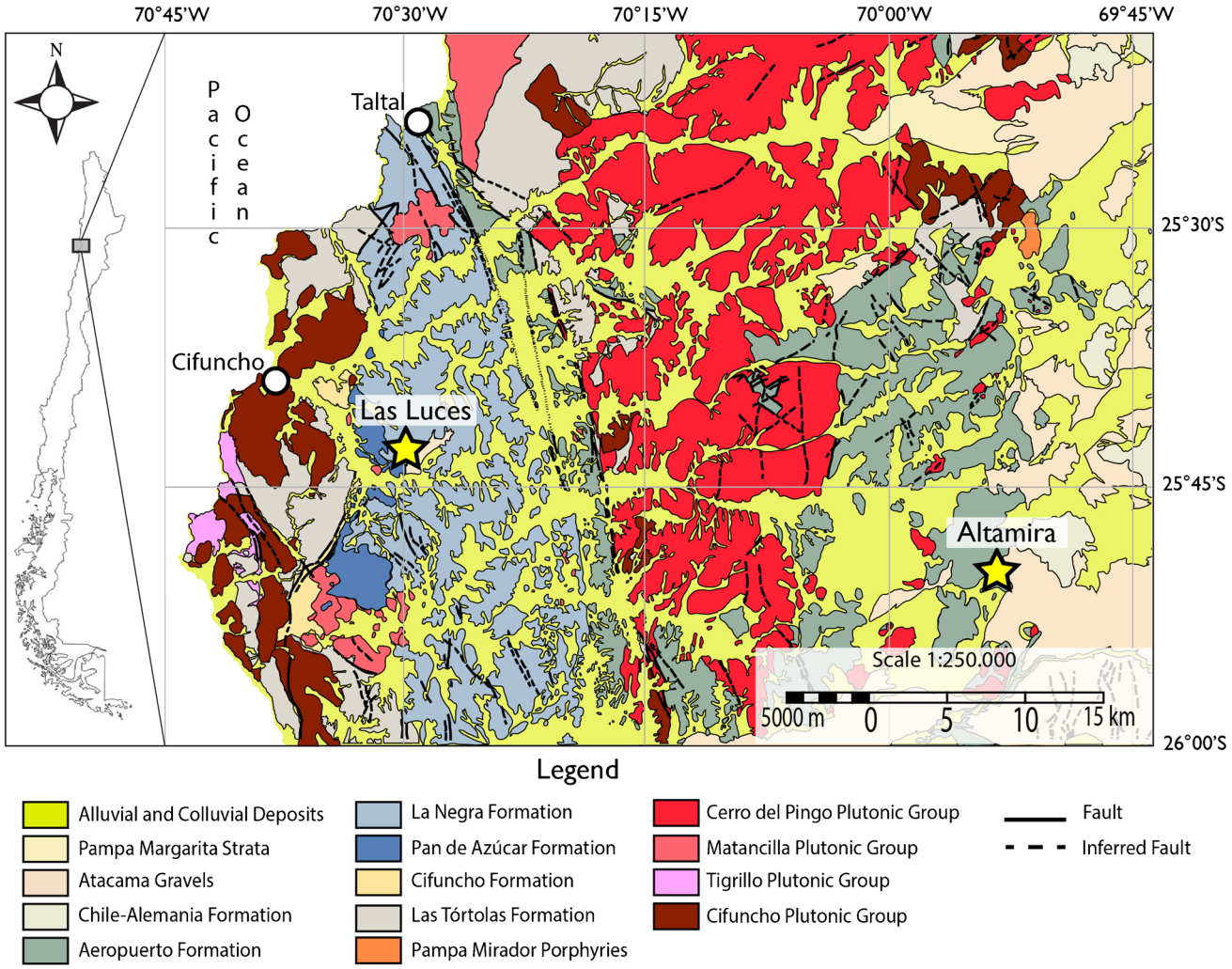

Fig. 2 Geologic map of the studied area. The main geological units, structures, and location of the Las Luces and Altamira deposits are shown. Modified from Naranjo and Puig (1984)

granites (e.g., Matancilla Plutonic Group, Fig. 2). Limited geochronological information indicates that the emplacement of the plutonic bodies occurred during two main periods (190–173 Ma and 160–142 Ma; Pichowiak et al. 1990; Boric et al. 1990; Maksaev 1990; Scheuber and González 1999; Maksaev and Zentilli 2002; Oliveros et al. 2006, 2008). Overlying the volcanic rocks of the La Negra Formation is the Early Cretaceous Aeropuerto Formation, which represents the arc/back arc transition. This formation comprises porphyritic andesites interbedded with andesitic tuffs and breccias, conglomerates, sedimentary breccias, sandstones, and locally fossiliferous limestones (Fig. 2; Naranjo and Puig 1984; Boric et al. 1990). Several plutonic bodies, ranging in composition from granite to monzodiorite and with K–Ar and $^{40}Ar/^{39}Ar$ ages between 136 and 109 Ma (Boric et al. 1990) intruded the La Negra and Aeropuerto formations. These felsic stocks have been grouped into the Cerro del Pingo Plutonic Group (Naranjo and Puig 1984; Fig. 2). The Upper Cretaceous-Eocene Chile-Alemania Formation comprises volcanic rocks of andesitic to dacitic composition and minor basalts and rhyolites (Boric et al. 1990). This sequence unconformably overlies the Aeropuerto Formation and underlies the polymictic and unconsolidated Atacama Gravels of Oligocene to Miocene age (Naranjo and Puig 1984; Sun et al. 2018). The youngest intrusive complex in the area is the Pampa Mirador Porphyries (78–75 Ma; Fig. 2) of rhyolitic composition. This unit intruded the Cifuncho Plutonic Group and the Aeropuerto Formation (Naranjo and Puig 1984). The Miocene–Pleistocene is represented by the Pampa Margarita Strata, which comprises sandstones, siltstones, shales, breccias and conglomerates, limestones, and tuffs (Boric et al. 1990).

The main structural system in the area is the Atacama Fault System (AFS), recognized with a NS orientation along the present-day Coastal Cordillera between 21 and

30°S (St. Amand and Allen 1960; Arabasz 1968; Scheuber and Andriessen 1990; Brown et al. 1993; Cembrano et al. 2005; González et al. 2006; Mitchell and Faulkner 2009). The AFS was developed during the Late Jurassic–Early Cretaceous as an intra-arc regional structure related to oblique subduction of the Aluk plate relative to the South American continent (Boric et al. 1990; Scheuber and González 1999; Cembrano et al. 2005). This system comprises a series of large NS striking, vertical to subvertical brittle structures more than 60 km long, formed by sinistral strike–slip movements (Hervé 1987; Scheuber and Andriessen 1990). Several secondary NW splay faults developed as a result of these movements forming strike–slip duplexes (Cembrano et al. 2005).

Geology of the Las Luces deposit

The Las Luces deposit is owned by Grupo Minero Las Cenizas and current resources are estimated at 2.3 Mt at 1.11% Cu (Zamora 2011a).

The deposit is located about 50 km SE from Taltal (Fig. 2) and is hosted in volcanic rocks of the La Negra Formation (ESM Fig. 1), which in the area is represented by basaltic andesite and andesitic lava flows, volcaniclastic layers, and minor volcanic breccias. The sequence forms a monocline fold with a NE trend and variable dip between 12 and 25° SE. The basaltic andesite and andesite rocks have porphyritic to aphanitic textures, frequently amygdaloidal, and the phenocrysts are composed mainly of plagioclase 1 to 5 mm in length, but in some cases up to 1 cm (Fig. 3A–D). The plagioclase phenocrysts constitute between 1 and 40% modal of the rock. Minor pyroxene microliths are recognized in a gray aphanitic groundmass associated with magnetite and plagioclase. The groundmass can sometimes be altered to red hematite (Fig. 3D). The plagioclase laths are generally replaced by albite and the pyroxene and magnetite grains are altered to chlorite and hematite, respectively. Chlorite, quartz, and calcite are identified as secondary minerals filling vesicles (Fig. 3B). Calcite is also present in late-stage veinlets and in breccias, sometimes with Cu sulfides (Fig. 3E, F).

The volcaniclastic rocks comprise sub-rounded to rounded clasts between < 1 and 10 cm in diameter of porphyritic to amygdaloidal andesite in an aphanitic matrix mostly altered to chlorite (Fig. 3G). The main intrusion in the area is an elongated diorite body with a NW orientation and a variable thickness between 30 and 80 m (Fig. 3H). The diorite is gray in color and has a fine-grained granular texture formed by albitized plagioclase and pyroxene crystals < 2 mm long, and minor hornblende altered to chlorite. Small grains of magnetite partially or totally replaced by hematite are observed in the groundmass. A gray trachy-andesite dike following the same NW orientation as the diorite is also observed in the district (ESM Fig. 1). The trachy-andesite is composed of small plagioclase phenocrysts (up to 2.5 mm long) partially altered to sericite and hornblende crystals replaced by chlorite in a groundmass of plagioclase microliths (up to 0.2 mm), quartz, and orthoclase. Small disseminated magnetite grains oxidized to hematite are also present. Minor andesite dikes with a main NW orientation have been described in the northern area of the district. Several hydrothermal breccia bodies are observed associated with the diorite intrusions. These breccias are clast supported with angular fragments of the andesite host rock and/or from the diorite dike. The cement is composed of calcite, minor quartz, and sparse sulfides (chalcopyrite ± pyrite; Fig. 3F).

The Las Luces area was affected by several strike–slip fault systems. The oldest set of faults is a NS system followed by a NW-NE conjugate system possibly developed as a duplex. The N30°W structures control the emplacement of the intrusive units (e.g., diorite, latite, and andesite dikes) in the district.

Geology of the Altamira district

The Altamira district is located 70 km SE of Taltal (Fig. 2). Three deposits are currently under exploitation in the district: Franke, previously known as Frankenstein mine, and China, both owned by KGHM International Ltd., and Altamira in operation by Grupo Minero Las Cenizas. Current resources estimated for the Franke and China deposits are at 8.3 Mt at 0.95% Cu (KGHM report 2015), whereas for Altamira total resources are estimated at 10.4 Mt at 1.2% Cu (sulfides) and 2.2 Mt with 1.8% Cu (oxides) (Zamora 2011b). A Cretaceous age has been inferred for the Altamira district based on the age of the Aeropuerto Formation and a Re–Os sulfide model age reported by Barra et al. (2017).

The ore deposits of the Altamira district are hosted by the Early Cretaceous Aeropuerto Formation (ESM Fig. 2), which is composed of three subunits (Naranjo and Puig 1984). The lower unit is formed by volcaniclastic breccias and red sandstones with an estimated thickness between 600 and 700 m. The middle unit comprises porphyritic, amygdaloidal, and aphanitic andesites interbedded with sandstones, tuffs, limestones, and shales (Fig. 4). The Cu mineralization is mainly found in andesites from this middle unit. The porphyritic andesite lavas have abundant plagioclase (20 to 30% modal) and scarce clinopyroxene phenocrysts (< 3% modal) (Fig. 4A, B). The groundmass is composed of plagioclase and clinopyroxene microliths associated with small grains of magnetite partially replaced by hematite. Amygdales 5–10 mm in diameter and filled with quartz, calcite, and chlorite are a common feature in the andesites. The thickness of this unit is variable between 30 and 200 m. The upper

unit, 30 to 45 m in thickness, includes alternating layers of limestones, calcareous sandstones, tuffs (Fig. 4C), and andesitic sills ranging from 5 to 10 m thickness. The area is covered by Upper Miocene to Pliocene rocks, mainly sandstones, siltstones, moderately consolidated sand gravels, alluvial sediments, and lesser amounts of tuffs. The thickness of this section ranges from 10 to 40 m.

The deposit is characterized by an upper Cu oxide zone grading downward to an intermediate mixed Cu-oxide + sulfide zone and hypogene copper mineralization at depth (Fig. 4D–F). The Altamira district is affected by NS and NNW-NW structures, which are crosscut by NNE-NE faults. The NS and NNW-NW structures are the main control of the copper mineralization forming a series of vein-fault ore bodies (Zamora 2011b).

Samples and methods

A total of 16 and 14 drill cores were logged and sampled in Las Luces and Altamira, respectively. Petrographic and ore mineralogy characterization was performed on representative samples in order to determine the paragenetic sequence of alteration and mineralization. Electron microprobe analyses of bornite and "chalcocite" were performed to determine the concentration of minor elements (i.e., Ag, As, Sb, Se, Te, Au, Ni, Co, and Hg) in these phases. The term "chalcocite" is used here indistinctively when referring to mineral species of the chalcocite (Cu_2S) series. The series includes yarrowite ($Cu_{1.12}S$), spionkopite ($Cu_{1.39}S$), geerite ($Cu_{1.6}S$), anilite ($Cu_{1.75}S$), digenite ($Cu_{1.8}S$), djurleite ($Cu_{1.95}S$), and chalcocite (Cu_2S). Bulk stable isotope analysis was carried

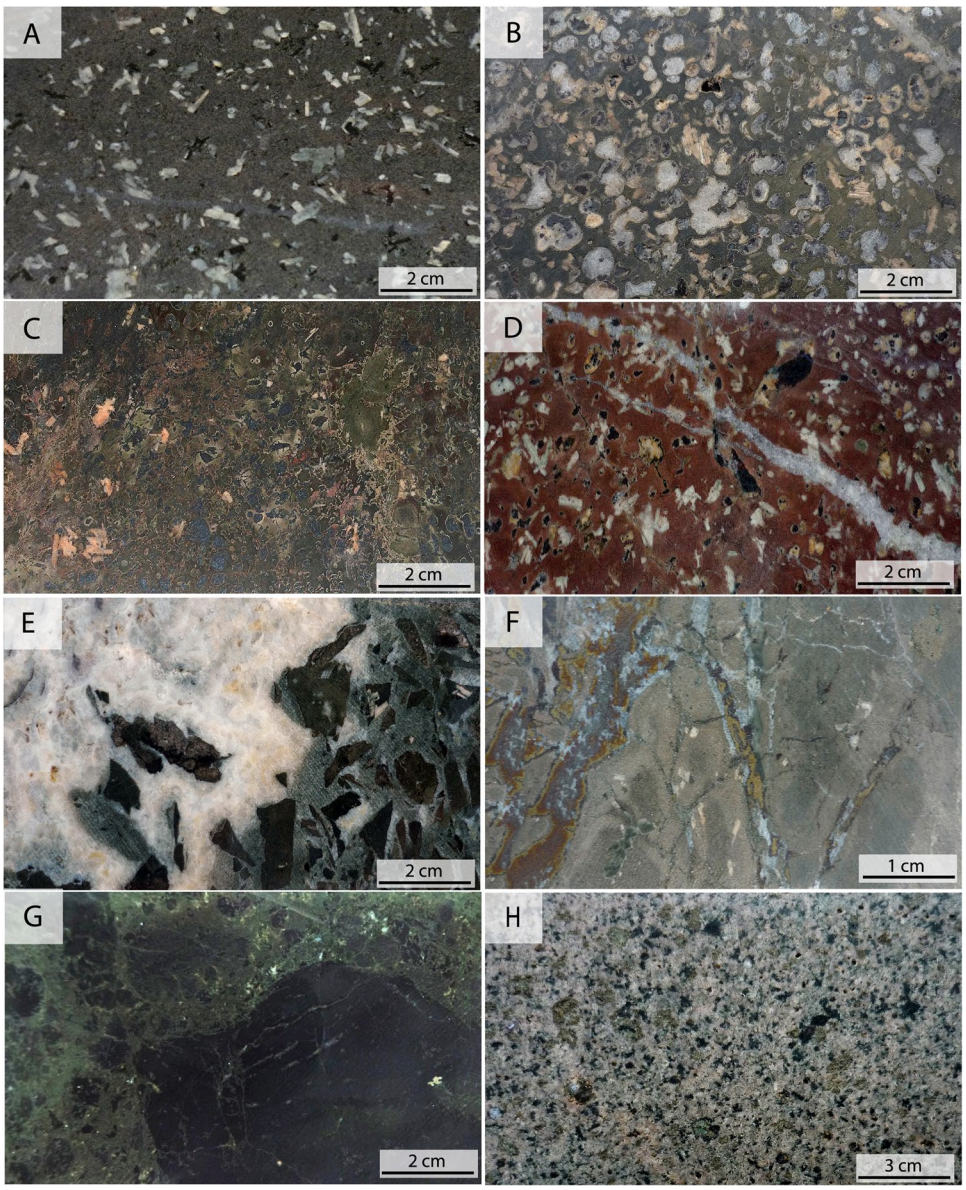

Fig. 3 Representative rock types in Las Luces. **A** Porphyritic unmineralized andesite with plagioclase phenocrysts pervasively altered to albite and minor sericite. Small pyroxene crystals partial or totally replaced by chlorite and hematite are also observed. **B** Porphyritic andesite with plagioclase phenocrysts altered to albite and amydules filled with calcite, quartz, and chalcocite. **C** Mineralized porphyritic andesite with albite phenocrysts partially altered to sericite and a groundmass dominated by a chlorite–hematite association. Also visible are irregular, disseminated black chalcocite grains. **D** Porphyritic andesite with plagioclase phenocrysts altered to albite in a groundmass pervasively altered to red hematite. Black chalcocite is observed as irregular grains within the groundmass. Late calcite veinlets crosscut the sample. **E** Hydrothermal breccia composed of porphyritic andesite clasts and a calcite–chlorite–quartz matrix. **F** Hydrothermal breccia with aphanitic andesite clasts in a matrix composed of calcite–chalcopyrite ± bornite ± chlorite. **G** Volcanoclastic rock composed of andesite clasts in a chlorite-rich matrix. **H** Diorite intrusion composed of pyroxene crystals partial or totally replaced by amphibole–chlorite–epidote and plagioclase grains totally altered to albite and minor sericite

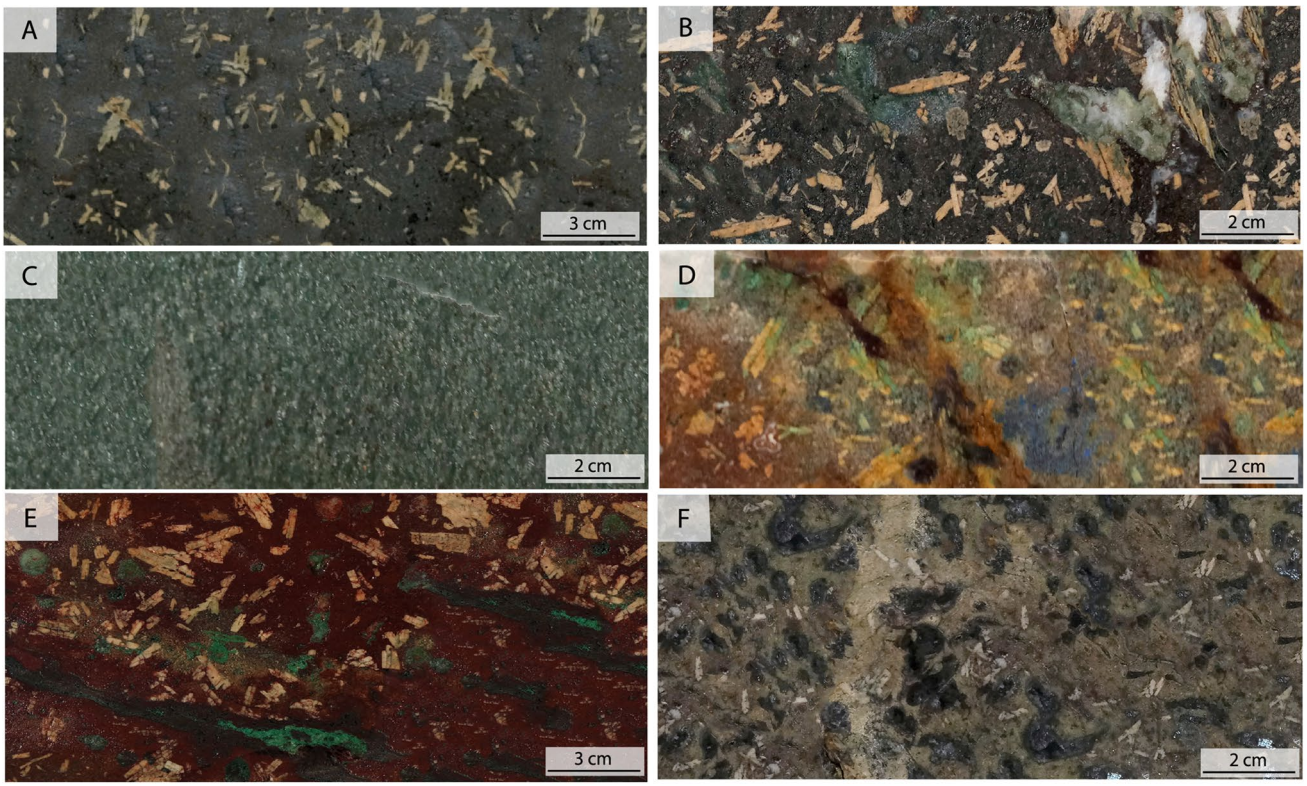

Fig. 4 Representative rock types and mineralization styles observed in Altamira. **A** Porphyritic andesite with plagioclase phenocrysts pervasively altered to albite immersed in a groundmass composed of albite and pyroxene microliths. Minor hematite and magnetite are also found in the groundmass. **B** Amygdaloidal andesite with albite and pyroxene phenocrysts in a groundmass partially hematitized with microliths of albite and pyroxene. Amygdules are filled with zeolite–prehnite–pumpellyite–chlorite–calcite ± chalcocite. **C** Lithic tuff with clasts of andesite in a groundmass pervasively altered to chlorite. **D** Porphyritic andesite with copper carbonates (azurite and malachite). **E** Porphyritic andesite from the upper oxidation zone showing pervasive hematitization of the groundmass, chalcocite veinlets partially oxidized to malachite, and/or atacamite. **F** Amygdaloidal andesite with pervasive sericitization of the groundmass. Amygdules are filled with chalcocite and minor bornite

out on sulfides (bornite, chalcocite, and pyrite) to establish the source of sulfur. Methods are summarized below.

SEM and EPMA methods

Scanning electron microscopy (SEM) observations were performed at the Andean Geothermal Center of Excellence (CEGA) Microanalysis Laboratory, Department of Geology, Universidad de Chile, by using a FEI Quanta 250 SEM equipped with a secondary electron (SE) and backscattered electron (BSE) detectors, and an energy-dispersive X-ray spectrometer. Energy-dispersive X-ray spectrometry (EDS) analyses were carried out on several sulfide phases in order to corroborate previous mineral identification by optical microscopy and to select areas within sulfides for electron microprobe analysis. The analytical parameters were spot-size set to 1–3 µm, accelerating voltage of 15 keV, beam intensity of 80 µA, and a working distance of ~ 10 mm.

Major and minor elements in sulfides were determined at the GeoAnalytical Laboratory, Washington State University, Pullman, USA, by using a JEOL JXA-8500F electron microprobe analyzer (EMPA). Operating conditions were 20 keV accelerating voltage and a 50-nA fully focused beam. Measured elements include Cu (Kα), Fe (Kα), Zn (Kα), Ni (Kα), Co (Kα), As (Lα), Sb (Lα), Ag (Lα), Au (Mα), Se (Lα), Bi (Mβ), S (Kα), Pb (Mα), Te (Lα), and Hg (Lα). The standards used for calibration were FeS_2 (for Fe), CuO (for Cu), FeAsS (for S and As), ZnS (for Zn), $(Ni,Fe)_9S_8$ (for Ni), HgS (for Hg), PbS (for Pb), Co^0 (for Co), Ag^0 (for Ag), $Bi_{12}GeO_{28}$ (for Bi), ZnSe (for Se), Sb_2S_3 (for Sb), Sb_2Te_3 (for Te), and Au^0 (for Au). Standards were tested for homogeneity before their use in quantitative analysis. Detections limits were 150 ppm (Zn), 360 ppm (Hg), 290 ppm (Pb), 140 ppm (Fe), 460 ppm (Co), 100 ppm (Ni), 220 ppm (Cu), 110 ppm (S), 180 ppm (As), 160 ppm (Se), 170 ppm (Sb), 180 ppm (Te), 170 ppm (Ag), 230 ppm (Au), and 260 ppm (Bi). Counting time was 10 s for Cu, Fe, and S; 30 s for Zn and Ni; 40 s for Hg; 50 s for Pb, Co, and Ag; 75 s for As, Se, Sb, and Te; and 100 s for Au.

Stable isotope analysis

Sulfur isotope analysis was carried out on bornite, chalcocite, and pyrite at the Environmental Isotope Laboratory of the Department of Geosciences, University of Arizona, Tucson, USA. A continuous-flow gas-ratio mass spectrometer (CF-IRMS) ThermoQuest Finningan Delta PlusXL model coupled with a Costech elemental analyzer was used for isotopic measurements. Samples were introduced into a combustion chamber with O_2 and V_2O_5 (Coleman and Moore 1978) to obtain a SO_2 gas at 1030 °C. The system was calibrated by using two international standards, the OGS-1 which is $BaSO_4$ precipitated from seawater and NBS123, a sphalerite sample with a $\delta^{34}S$ value of + 17.09‰. A linear calibration between − 10 and + 30‰ was performed and a precision of ± 0.15 (1σ) was estimated by measurement of several internal standards (http://www.geo.arizona.edu/node/153). Data are reported in the δ notation in per mil (‰) relative to the Canyon Diablo Troilite (CDT) standard: $\delta^{34}S = [(^{34}S/^{32}S)_{sample}/(^{34}S/\ ^{32}S)_{standard} - 1] \times 1000$.

Results

Alteration and mineralization

Las Luces deposit

The volcanic host rocks in Las Luces have porphyritic and amygdaloidal with minor aphanitic textures (Fig. 3). The porphyritic andesite comprises plagioclase (10–40% modal) and lesser pyroxene (< 10% modal) phenocrysts. The groundmass is composed of plagioclase and pyroxene microliths. The volcanic rocks have been affected by a regional burial low-grade metamorphism represented by zeolites, prehnite–pumpellyite, and chlorite (Losert 1973; Palacios and Definis 1981; Sato 1984). The hydrothermal alteration that affected the volcanic rocks overprints this metamorphic assemblage and is characterized by selective albitization of primary plagioclase. Sericite is observed as an alteration product of albitized plagioclase (Fig. 5A, B). Calcite is present as amygdale fillings, associated with chlorite–smectite, and also in veinlets (Fig. 5C, D), sometimes with Cu-bearing sulfides. Chlorite, epidote, quartz, and smectite are also found filling amygdales (Fig. 5E, F). Hematite, quartz, and goethite are observed in the groundmass.

The hypogene Cu mineralization is usually observed as disseminated grains, in amygdales, veinlets, and in the matrix of hydrothermal breccias (Fig. 6). The mineralization event can be divided in two main stages: hypogene and supergene.

i) The hypogene stage consists of two substages, i.e., pre-ore and main-ore. The former is characterized by pyrite and minor chalcopyrite, and large crystals of hematite (Fig. 6A). Pyrite crystals are irregular in shape and can be replaced by chalcopyrite through fractures (Fig. 6B). The main-ore substage consists of a bornite and chalcocite association with a myrmekitic-type intergrowth texture (Fig. 6C). Lesser amounts of chalcopyrite are related to local hydrothermal breccias with calcite and can be replaced by bornite (Fig. 6D). Lastly, hematite is present as small aggregates, generally surrounding amygdales and veinlets in which Cu sulfides are present (Fig. 6F).

ii) The supergene stage is characterized by the formation of digenite/covellite replacing hypogene bornite and chalcocite through grain rims and along fractures (Fig. 6D). In addition, minor quantities of azurite and malachite are observed close to fractures (Fig. 6E). The paragenetic sequence for the Las Luces deposit is shown in Fig. 7.

Altamira deposit

The volcanic rocks that host the Cu–(Ag) mineralization in Altamira are composed of plagioclase and scarce pyroxene phenocrysts (< 5% modal) in a fine-grained groundmass of plagioclase and pyroxene microliths and small magnetite crystals. Similar textures as those described for Las Luces are also present in Altamira, i.e., porphyritic, aphanitic, and amygdaloidal. The very-low- to low-grade metamorphic assemblage is represented by prehnite–pumpellyite and minor amounts of zeolites and chlorite–smectite, whereas the hydrothermal alteration paragenesis comprises albite (Fig. 8A), chlorite, calcite, and minor clays, quartz, and sericite. Amygdales are filled with chlorite, quartz, and calcite as well as prehnite, pumpellyite, and locally zeolites (Figs. 8B–F) in close association with Cu sulfides.

The hypogene copper mineralization is usually observed as disseminated grains, amygdale infillings, and veinlets. Mineralization in the deposit is divided in three stages: diagenetic, hypogene, and supergene.

i) The diagenetic stage is characterized by the formation of framboidal pyrite, with typical spheroidal textures replaced by chalcocite/digenite and covellite (Fig. 9A, B).

ii) The hypogene stage (main hydrothermal event) can be further subdivided in two substages: an early pre-ore and a main-ore substage. The pre-ore substage is characterized by the presence of small disseminated pyrite grains and veinlets. In addition, small disseminated primary magnetite crystals are observed partially replaced by hematite. The main-ore stage consists of Cu sulfides with scarce bornite and chalcopyrite (Fig. 9C).

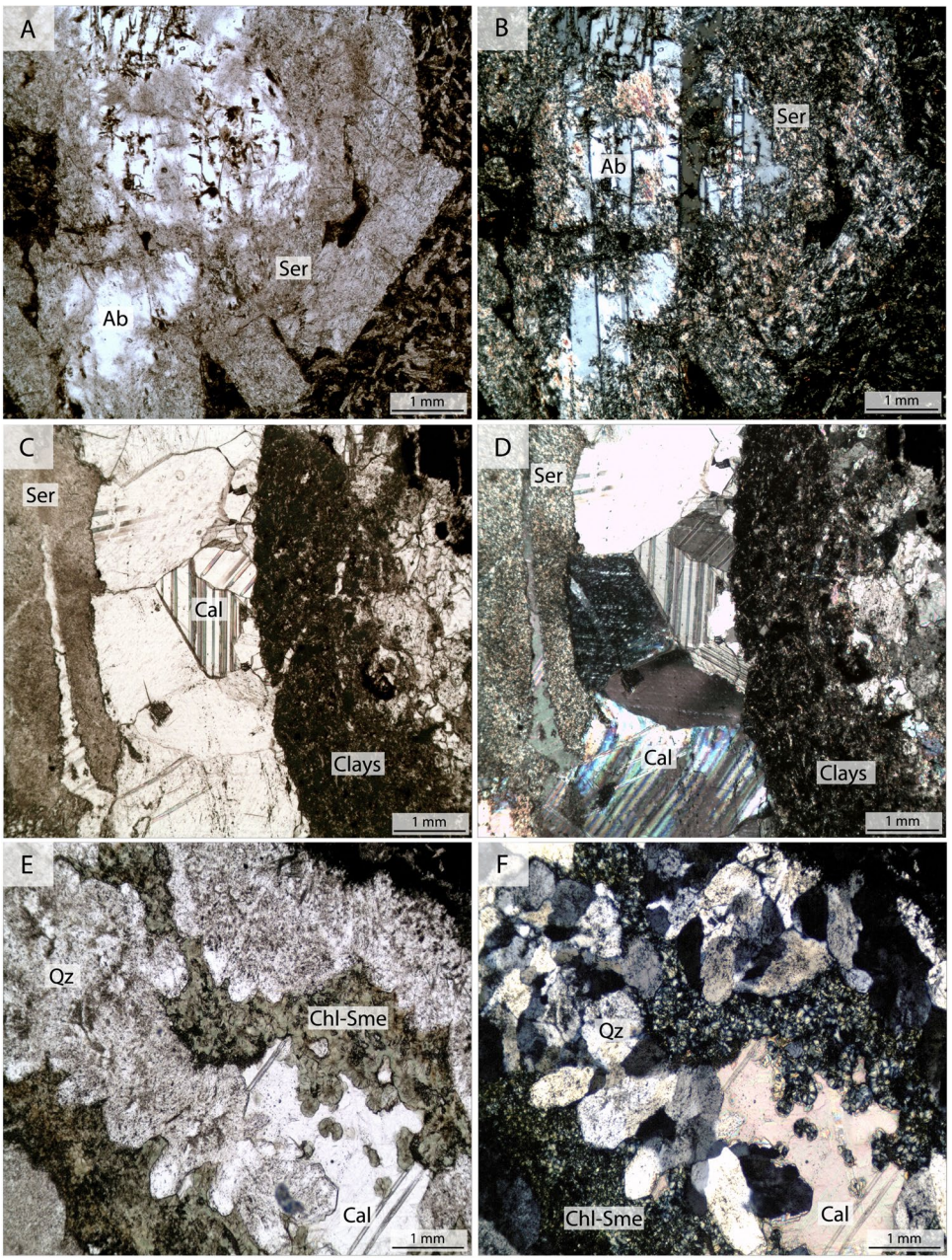

Fig. 5 Alteration minerals from Las Luces. **A**, **B** Glomeroporphyritic texture of albitized plagioclase phenocrysts exhibiting pervasive sericitic alteration. **C**, **D** Calcite veinlet with a sericite–clay halo. **E**, **F** Amygdule filled with calcite–quartz–chlorite/smectite. Ab, albite; Cal, calcite; Chl-Sme, chlorite–smectite; Qz, quartz; Ser, sericite

iii) The supergene stage is represented by the formation of minor secondary chalcocite and covellite—which replaced bornite and primary Cu sulfides through grain rims and along fractures (Fig. 9D)—and chrysocolla, Cu carbonates (azurite and malachite), and minor atacamite in the upper oxidation zone (Fig. 9E). The paragenetic sequence for Altamira is shown in Fig. 10.

Micron-size particles of a Ag-bearing sulfide were identified under the SEM. These particles are observed attached or close to digenite rims. In addition, the small-size (< 10 µm) framboidal pyrite grains were further investigated by using the SEM, showing a partial to total replacement by Cu sulfides (Fig. 11).

Mineral chemistry

Electron microprobe analyses for Las Luces and Altamira are summarized in Table 2. All data is presented in the Electronic Supplemental Material file. Mostly all trace elements (As, Sb, Se, Te, Au, Ni, Hg), with the exception of Ag and Co, are at or below detection limits. Figure 12 shows the Cu and Ag contents for the analyzed sulfide phases.

Chalcocite

The Cu content in Las Luces "chalcocite" ranges between 77.2 and 78.9 wt% and sulfur from 20.3 to 21.8 wt%,

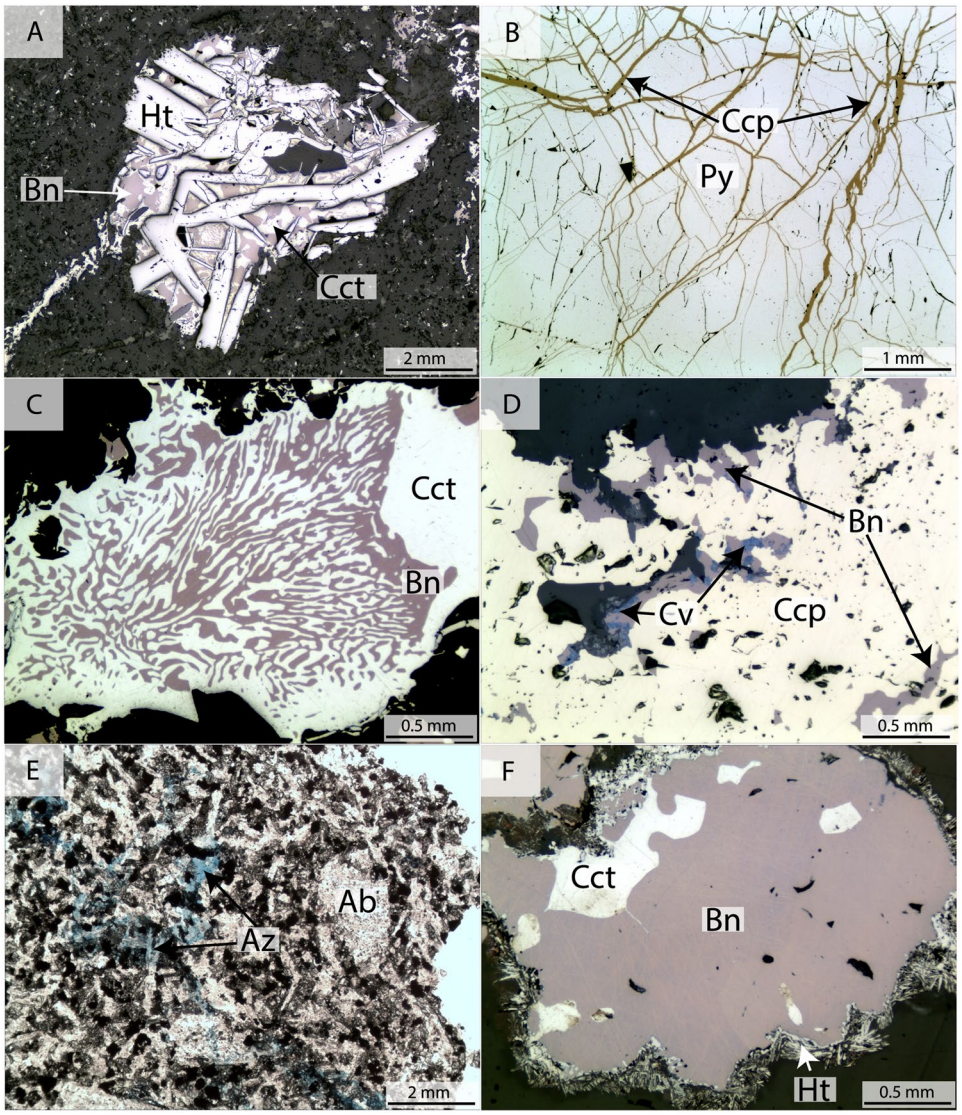

Fig. 6 Photomicrographs of ore minerals from Las Luces. **A** Bornite- "chalcocite" with a myrmekitic-type texture and intergrown with large hematite crystals. **B** Large pyrite grain replaced by chalcopyrite along fractures. **C** Typical myrmekitic-type texture of bornite in "chalcocite." **D** Chalcopyrite partially replaced by bornite through rims and fractures followed by bornite replaced by covellite. **E** Late oxidation event is illustrated by the presence of azurite. **F** Amygdale filled with bornite and "chalcocite." Small acicular hematite crystals are observed surrounding the amydule. Ab, albite; Az, azurite; Bn, bornite; Cct, chalcocite; Ccp, chalcopyrite; Cv, covellite; Hem, hematite; Py, pyrite

whereas in Altamira is from 73.6 to 78.2 and 20.6 to 22.8 wt%, respectively (Table 2). Copper deficiency is notorious in all analyzed spots ($n = 60$), with a mean of 1.79 atoms per formula unit (apfu) of Cu per each S in Altamira ($Cu_{1.79}S$), whereas for Las Luces this value is 1.85 of Cu per each S ($Cu_{1.85}S$). For these compositional ranges, the mineral phases analyzed fit within digenite–djurleite for Las Luces and geerite–digenite in Altamira (Fig. 13). Iron concentration in Las Luces Cu sulfides is < 0.52 wt%, whereas in Altamira is < 1.73 wt%. The Ag content in Las Luces chalcocite is less than 0.27 wt%, with a mean value of 0.08 wt%. Silver values in chalcocite from Altamira are much higher, reaching up to 0.79 wt%, with a mean value of 0.15 wt% (Table 2). Cobalt was detected in all Cu sulfide samples with concentrations from 0.05 to 0.14 wt%.

Bornite

Cu, S, and Fe concentrations in bornite from Las Luces range from 61.1 to 68.5 wt%, 22.5 to 26.3 wt%, and 8.4 to 11.1 wt%, respectively. Bornite is scarce in Altamira and only one analysis is reported in Table 2. Silver and Co values in Las Luces bornites range between 0.02 and 0.27 and 0.04 and 0.12 wt%, respectively. These Ag and Co values are similar to those reported for "chalcocite."

Sulfur isotope data

Nine sulfide-bearing samples from the Altamira and Las Luces deposits were analyzed using bulk sulfur isotope analysis. Sulfates are not present in these deposits. The $\delta^{34}S$

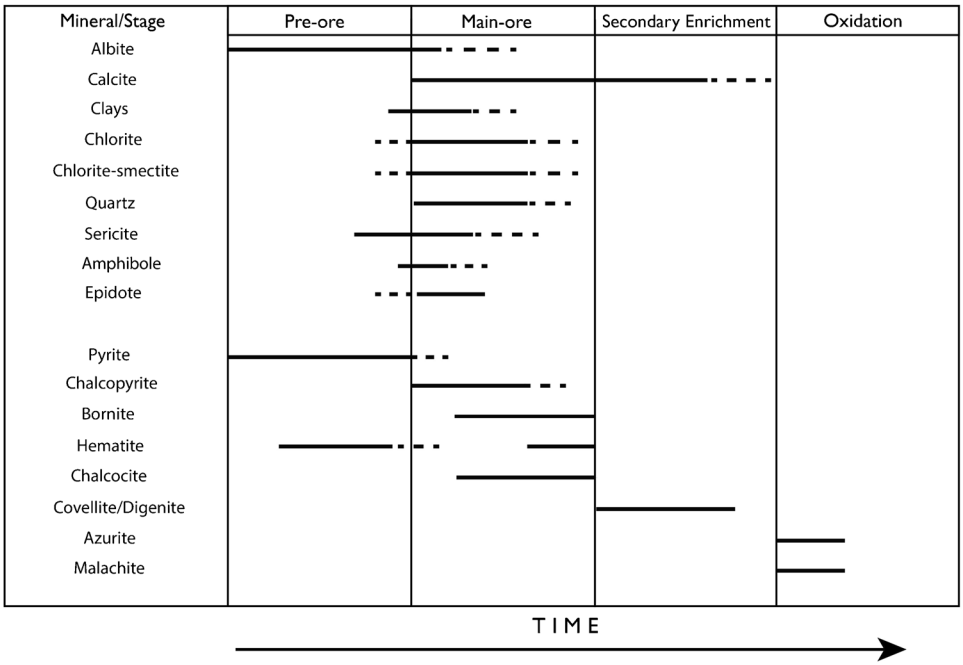

Fig. 7 Paragenetic sequence for Las Luces ore deposit

values obtained for sulfides range from –2.5 to + 2.9‰ in Las Luces and –38.7 to –10.7‰ in Altamira (Table 3).

Discussion

Mineralization and alteration

The alteration assemblage observed in both Las Luces and Altamira is characterized by a typical sodic (albite) and propylitic alteration with chlorite and late calcite (Figs. 5 and 8). This alteration assemblage indicates formation by near neutral pH fluids. The occurrence of prehnite–pumpellyite–chlorite filling amygdales from the volcanic rocks of the Aeropuerto Formation indicates that the Altamira host rocks were affected by burial metamorphism, as it has been also documented for most of the Cretaceous stratabound deposits (Losert 1973; Boric et al. 2002; Cisternas and Hermosilla 2006; Carrillo-Rosúa et al. 2014).

Mineralization at Las Luces and Altamira is similar to that described in other stratabound Cu–(Ag) deposits in Chile (Maksaev and Zentilli 2002; Kojima et al. 2003; 2009) with a pre-ore mineralization episode characterized by ubiquitous, fine-grained magnetite related to the volcanic host rocks, and minor pyrite followed by the formation of chalcopyrite (Figs. 7 and 10). Framboidal pyrite has been reported for Cretaceous deposits in central Chile (Fig. 1) and has been interpreted as formed by bacterial seawater sulfate reduction during early diagenesis (Wilson et al. 2003b). In several Cretaceous deposits, the presence of bitumen and/or pyrobitumen has been reported (Cisternas and Hermosilla 2006; Herazo et al. 2020); however, to date no residual hydrocarbons have been identified in Altamira.

The main copper event consists of chalcocite-series minerals ranging from geerite to djurleite and variable amounts of bornite. A supergene event that formed secondary covellite and copper oxides (e.g., azurite, malachite, atacamite, chrysocolla) has been observed in both deposits, however, of limited extension. The scarce presence of pyrite and hence of sulfuric acid produced by the oxidation of pyrite under supergene conditions is probably the cause for the poorly developed supergene oxide zone.

The bornite–digenite solid solution: implications for estimates of temperature of ore formation

The bornite–Cu sulfide myrmekite-like exsolution texture (Fig. 6) is a common feature observed in Chilean manto-type deposits (Kojima et al. 2003; Tristá-Aguilera et al. 2006; Ramírez et al. 2006; this study). Textural information of sulfides, particularly exsolutions, can provide information on the thermal history of the mineral assemblage; however, most of the ore mineral assemblages suffer rapid transformations as they re-equilibrate under changing temperature conditions, i.e., cooling (Grguric and Putnis 1999). Bornite and digenite form a solid solution at temperatures above 265 °C and upon cooling the bornite end-member undergoes phase transitions where the low bornite phase, stable at < 190 °C, is the only natural occurring polymorph (Grguric et al. 2000). On the other hand, the phase relations in the Cu–S diagram are more complex with several phases including djurleite ($Cu_{1.97}S$), digenite ($Cu_{1.80}S$), roxbyite

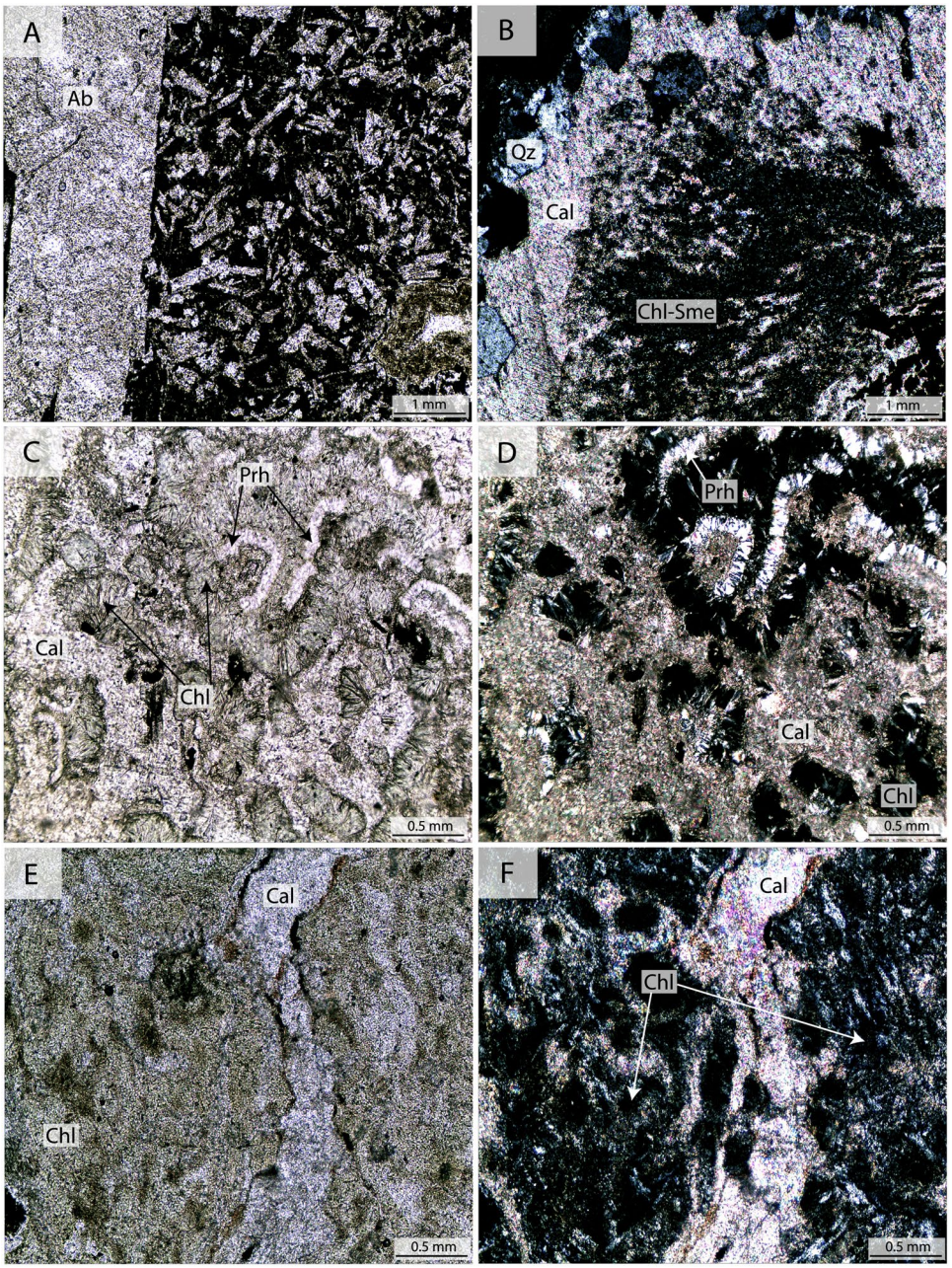

Fig. 8 Representative photomicrographs of alteration minerals in the Altamira host rocks. **A** Porphyritic andesite with a large plagioclase phenocryst pervasively altered to albite and immersed in a groundmass composed by albite microliths. **B** An amygdule filled with chlorite/smectite–calcite and quartz. **C** Amygdule filled with prehnite, chlorite, and calcite. **D** Same as in **C** but with crossed nicols. **E** Amygdule filled with chlorite crosscut by a late calcite veinlet. **F** Same as in **E** but with crossed nicols. Ab, albite; Cal, calcite; Chl, chlorite; Chl-Sme, chlorite–smectite; Prh, prehnite; Ser, sericite

($Cu_{1.78}S$), anilite ($Cu_{1.75}S$), geerite, ($Cu_{1.60}S$), spionokopite, ($Cu_{1.40}S$), and yarrowite (Cu_9S_8) (Fleet 2006). The revised phase diagram for the bornite–digenite join proposed by Grguric et al. (2000) supports a minimum formation temperature of 83 °C for the bornite– "chalcocite" myrmekite-like texture. Further, the presence of several low-temperature Cu–S phases (Fig. 13) is also indicative of re-equilibration at temperatures below 100 °C for the main Cu ore stage, although these estimates should be considered with caution due to the limited experimental work on the stability of these low-temperature phases and the effects of Ag (and Fe) substitution in "chalcocite."

Overall, a low formation temperature is consistent with fluid inclusion data (Th < 300 °C) for some manto deposits (Oyarzún et al. 1998; Kojima et al. 2003; Saric et al. 2003; Cisternas and Hermosilla 2006; Rieger et al. 2008), and more recent studies based on the trace-element content (Ag–Co–Cu) in pyrite (Herazo et al. 2021).

Silver content in Cu–(Fe) sulfides

Trace elements in bornite and Cu sulfides are below detection limits with the exception of Ag and Co, and Fe in "chalcocite" (Table 2). It is well known that Ag is an important

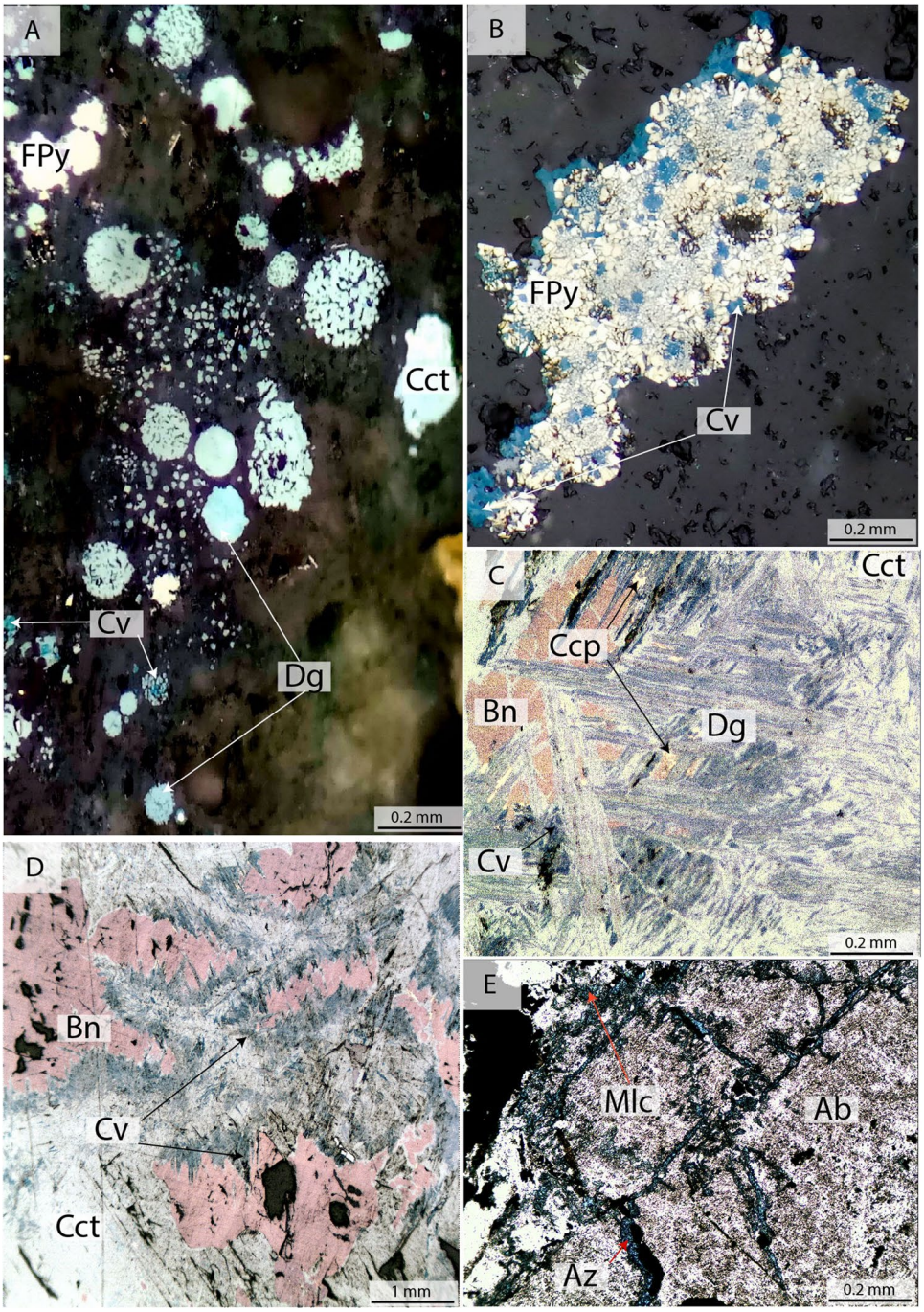

Fig. 9 Photomicrographs of ore minerals from the Altamira deposit. **A** Framboidal pyrite replaced by chalcocite/digenite. **B** Framboidal pyrite aggregates replaced by covellite. **C** Hypogene chalcopyrite–bornite– "chalcocite" association replaced by digenite and covellite. **D** Secondary covellite replacement along the contact between "chalcocite" and bornite. **E** Plagioclase phenocryst crosscut by azurite–malachite veinlets. Ab, albite; Az, azurite; Bn, bornite; Cct, chalcocite; Ccp, chalcopyrite; Cv, covellite; Dg, digenite; FPy, framboidal pyrite; Mlc, malachite

by-product of Cu mining of Chilean manto-type deposits, but to the date, there is scarce information on the speciation and mineralogical form of Ag in hypogene copper sulfides, i.e., in solid solution in the Cu–(Fe) sulfide structure or as micro- to nanosized particles or inclusions of native Ag or Ag sulfides or tellurides. The data obtained from the studied sulfides shows that a considerable amount of Ag is incorporated in Cu sulfides, ranging from 200 to 2100 ppm in Las Luces and 228 to 7886 ppm in Altamira (Fig. 12, Table 2). In addition, bornite from Las Luces can also contain high amounts of Ag (226–2675 ppm). Bornite is scarce in Altamira and only one data point is reported in Table 2.

Previous studies on the incorporation of Ag (and Au) in supergene digenite from Mantos de la Luna, Michilla, and Mantos Blancos (Fig. 1) show that their Ag concentration is strongly correlated with the As content (Reich et al. 2010). Furthermore, digenite analyses with a Ag/As ratio > 30 are indicative of Ag nanoparticles as determined by SIMS depth profiling and TEM observations (Reich et al. 2010). Arsenic concentrations in Cu–(Fe) sulfides from Las Luces and

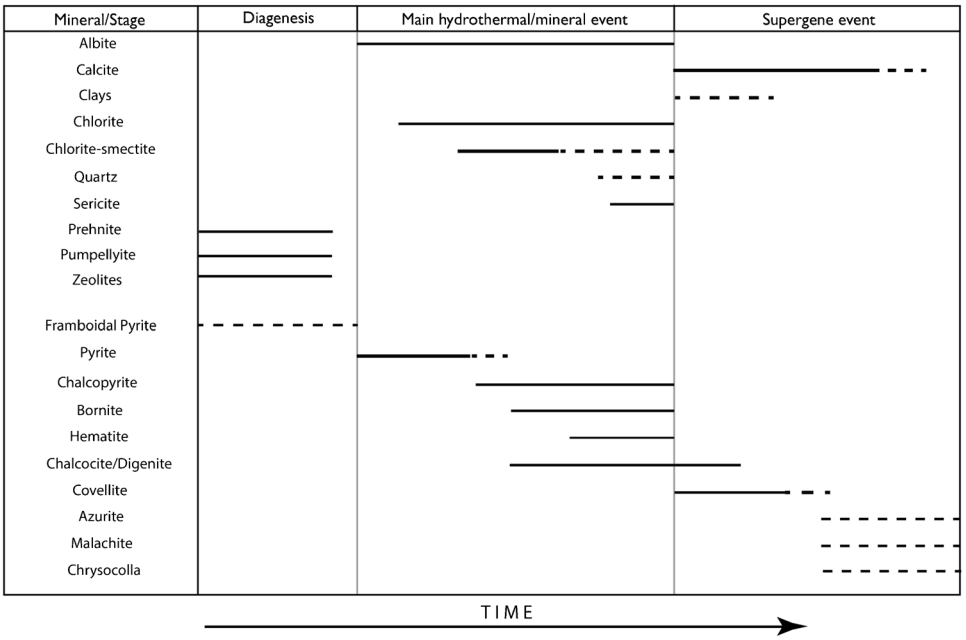

Fig. 10 Paragenetic sequence for the Altamira deposit

Altamira are mostly below EMPA detection limits (200 ppm; Table 2), and although the As concentration was not directly determined using SIMS or laser ablation ICP-MS, some general considerations can be discussed. The apparent lack of correspondence between Ag and As in the studied samples supports the notion that supergene chalcocite can have a different trace-element geochemical signature compared to hypogene chalcocite (Cook et al. 2011). However, if we consider 200 ppm—the EPMA detection limit for As—as the maximum As content in hypogene "chalcocite," calculated Ag/As ratios yield values of < 12, suggesting that Ag is mostly incorporated in solid solution within the "chalcocite" structure (Reich et al. 2010). This is consistent with the scarce presence of micron-sized Ag-bearing particles within the analyzed phases under SEM or EPMA, but the high content (up to 7900 ppm) in some Cu sulfide grains could be related to the presence of "invisible" nanosized Ag-bearing particles, as reported for supergene digenite from Michilla and Mantos de La Luna (Reich et al. 2010). The presence of rare, small Ag-rich sulfide aggregates in Altamira (Fig. 11) can be interpreted as a "Ag supergene enrichment" by dissolution of primary Cu–(Fe) sulfides or produced by local Ag supersaturation in the hydrothermal fluids.

Bornite is a major host of Ag in several ore deposit types where it generally can reach up to a few 100 ppm (Cook et al. 2011; Reich et al. 2013; Cioacă et al. 2014; Crespo et al. 2018, 2020; Liu et al. 2020). In porphyry Cu systems, Ag is mostly incorporated in solid solution in bornite, chalcopyrite, and Cu sulfosalts (tennantite, tetrahedrite, and enargite), but the presence of Ag-bearing particles has also been reported (Cook et al. 2011; Crespo et al. 2020). In addition, recent studies of sulfides

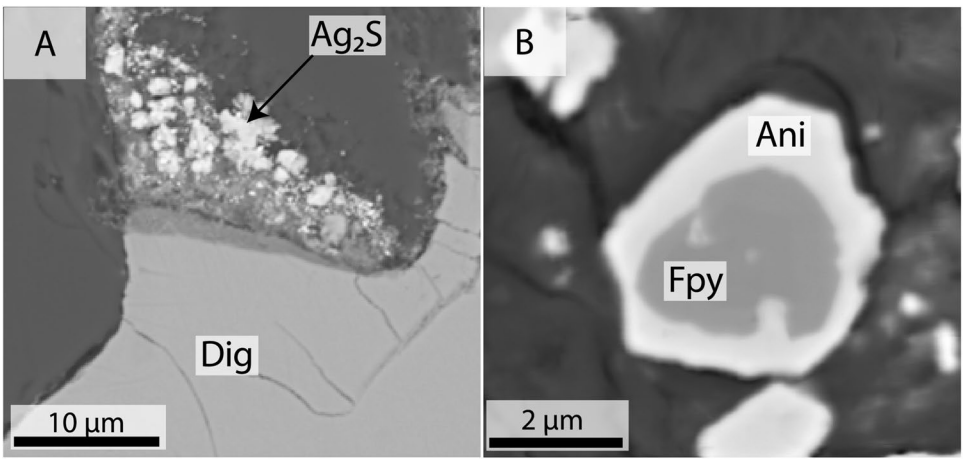

Fig. 11 Scanning electron microscope (SEM) images. **A** Acanthite microparticles associated with a digenite grain. **B** A micron-size framboidal pyrite relict replaced by anilite

Table 2 Summary of electron probe microanalysis (EMPA) data (in wt%) for Altamira and Las Luces. Detection limits (D.L.) are indicated for each element. b.d.l = below detection limits. The number of points above D.L is represented by *n*

		Deposit	Altamira					Las Luces				
Element	D.L	mineral	*n*	Mean	Min	Max	Median	*n*	Mean	Min	Max	Median
Cu	0.02	Bornite	1	-	-	62.33	-	39	66.04	61.14	68.46	66.69
		"Chalcocite"	28	75.81	73.63	78.20	75.65	32	77.86	77.17	78.76	77.80
Ag	0.02	Bornite	1	-	-	0.02	-	39	0.13	0.02	0.27	0.10
		"Chalcocite"	28	0.15	0.02	0.79	0.09	31	0.08	0.02	0.21	0.06
Fe	0.01	Bornite	1	-	-	10.68	-	39	9.27	8.41	11.12	9.02
		"Chalcocite"	26	0.81	0.03	1.73	0.69	30	0.17	0.02	0.52	0.11
S	0.01	Bornite	1	-	-	25.43	-	39	24.53	22.54	26.30	24.55
		"Chalcocite"	28	21.61	20.57	22.84	21.64	32	21.25	20.33	21.81	21.36
As	0.02	Bornite	0	-	b.d.l	b.d.l	-	3	0.02	0.02	0.02	0.02
		"Chalcocite"	4	-	0.03	0.08	-	1	-	-	0.02	-
Sb	0.02	Bornite	0	-	b.d.l	b.d.l	-	0	-	b.d.l	b.d.l	-
		"Chalcocite"	3	-	0.02	0.05	-	0	-	b.d.l	b.d.l	-
Se	0.02	Bornite	0	-	b.d.l	b.d.l	-	7	-	0.02	0.02	-
		"Chalcocite"	6	-	0.02	0.02	-	3	-	0.02	0.02	-
Te	0.02	Bornite	0	-	b.d.l	b.d.l	-	1	-	-	0.02	-
		"Chalcocite"	4	-	0.02	0.02	-	0	-	b.d.l	b.d.l	-
Au	0.02	Bornite	0	-	b.d.l	b.d.l	-	2	-	0.02	0.02	-
		"Chalcocite"	1	-	-	0.03	-	1	-	-	0.03	-
Ni	0.01	Bornite	0	-	b.d.l	b.d.l	-	3	-	0.01	0.01	-
		"Chalcocite"	5	-	0.01	0.02	-	6	-	0.01	0.02	-
Co	0.04	Bornite	1	-	b.d.l	b.d.l	-	36	0.08	0.04	0.12	0.08
		"Chalcocite"	28	0.08	0.05	0.14	0.08	32	0.09	0.06	0.13	0.09
Hg	0.04	Bornite	1	-	-	0.04	-	9	-	0.04	0.05	-
		"Chalcocite"	10	-	0.04	0.06	-	8	-	0.04	0.05	-

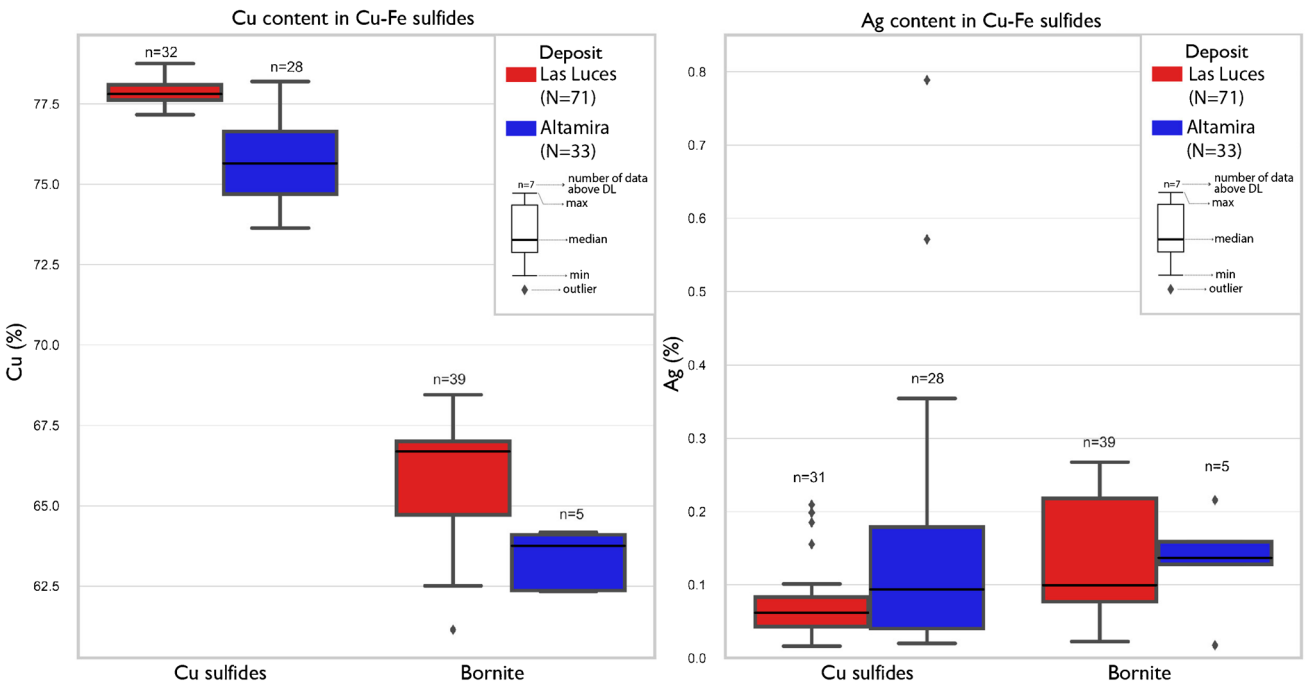

Fig. 12 Concentration box plots for Cu and Ag in Cu sulfides (chalcocite–covellite series) and bornite for Las Luces and Altamira

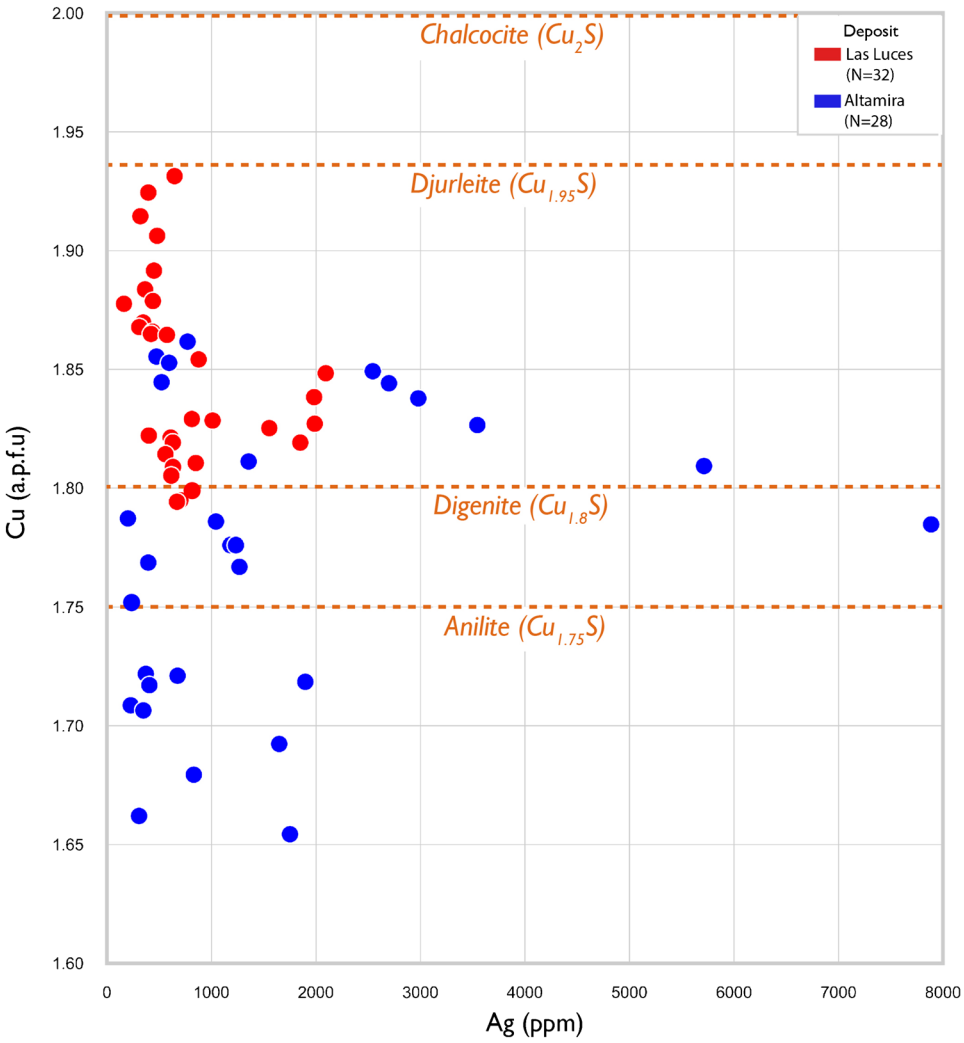

Fig. 13 Compositional range of Cu sulfides measured by EPMA for Altamira (blue) and Las Luces (red) versus the Ag content in ppm. The average formulas of 32 representative point analyses ($Cu_{1.85}S$) for Las Luces fall within the range of digenite-type solid solution series. For the Altamira deposit, the average apfu of Cu of 29 representative point analyses ($Cu_{1.77}S$) fits within the analite/digenite-type solid solution series (Will et al. 2002; Reich et al. 2010)

from the Rio Blanco porphyry Cu deposit show that Ag concentrations are highest in the high-temperature (~ 550 °C), early potassic alteration, and lowest in the distal propylitic alteration zone (Crespo et al. 2020). Furthermore, when chalcocite/digenite occurs in the mineral paragenesis along with bornite, the former preferentially concentrates Ag in comparison with the latter (Rivas et al. 2021). These data show that Ag incorporation in Cu–(Fe) sulfides is complex and subjected to several controlling factors, most importantly temperature and the presence of co-crystallizing Cu sulfide phases.

The incorporation of elements such as As, Sb, Bi, or Te may increase the precious metal content in Cu–(Fe) sulfides by a coupled substitution mechanism due to the higher ionic radii of Ag^+ (0.1 nm) in comparison with Cu^+ (0.6 nm) in tetrahedral coordination (Reich et al. 2010, 2013). A similar substitution mechanism could also explain the high amounts of Co (and Fe) reported for the analyzed Cu–(Fe) sulfides, where Co^+ and Fe^{+2} have similar ionic radii as Cu +, i.e., 0.58 and 0.63 nm, respectively, in tetrahedral coordination (Shannon 1976). However, further studies are needed to experimentally constrain the speciation and mineralogical occurrence of silver (nanoparticles?) and associated trace elements in bornite.

Table 3 Stable isotope analyses of the two studied deposits

Sample	Mineral phase	Occurrence	$\delta^{34}S$ (‰)
AL-S1	Chalcocite	Veinlet	–34.8
AL-S2	Chalcocite	Veinlet	–37.2
AL-S3	Chalcocite	Veinlet	–10.7
AL-S4	Chalcocite	Massive	–38.7
AL-S5	Chalcocite	Veinlet	–35.8
LL-S1	Bornite	Disseminated	+2.9
LL-S2	Pyrite	Amygdule filling	–1.2
LL-S3	Pyrite	Amygdule filling	–2.5
LL-S4	Pyrite	Amygdule filling	–2.1

AL, Altamira; *LL*, Las Luces

Source of sulfur

The sulfur isotope data obtained here reveal two distinct trends for the studied deposits: a restricted range of $\delta^{34}S$ values for Las Luces (–2.5 to + 2.9‰) and a wide range of light $\delta^{34}S$ values for Altamira (–10.7 to –38.7‰, Table 3). The $\delta^{34}S$ values of the primary Cu sulfides in Las Luces show that sulfur was most likely derived from an igneous source, either from the crystallizing intrusions or derived from leaching of the volcanic rocks. This is consistent with $\delta^{34}S$ values reported for other Jurassic stratabound Cu–(Ag) deposits (Kojima et al. 2009; Table 4).

On the other hand, highly negative $\delta^{34}S$ values have been reported for several Cretaceous deposits (Table 4), which indicate that sulfur was derived from bacteriogenic seawater sulfate reduction or by thermochemical sulfate reduction (Carrillo-Rosúa et al. 2014). Furthermore, the presence of framboidal pyrite has also been documented in these stratabound deposits where they are formed within and around liquid petroleum by bacterial degradation (e.g., Wilson and Zentilli 1999; Wilson et al. 2003b; Carrillo-Rosúa et al. 2014). No bitumen has been reported in the Altamira deposit, but considering the highly negative $\delta^{34}S$ values obtained in the analyzed samples and the fact that the Aeropuerto Formation has sedimentary units (Boric et al. 1990), it is plausible that both these sedimentary rocks and diagenetic pyrite, formed under anoxic conditions, are an important source of sulfur for the copper mineralization.

The similar characteristics between the Altamira deposit and the Lower Cretaceous stratabound deposits of central Chile, i.e., the extremely light sulfur isotope values, the presence of framboidal textures, the significant sedimentary component of the Aeropuerto Formation, and the Late Cretaceous Re–Os chalcocite model age reported in Barra et al. (2017), support an extension of the Cretaceous stratabound Cu–(Ag) belt further north of Copiapó (Fig. 1).

Table 4 Summary of stable isotope analyses for the main stratabound Cu–(Ag) deposits

	Deposit	Mineral phase	$\delta^{34}S$ (‰)	References
Jurassic Belt	Buena Esperanza	Copper concentrate	–0.3	Sasaki et al. (1984)
	Mantos de La Luna	Cct–Dg	–2.1 to –1.6	Kojima et al. (2009)
	Mantos del Pacífico	Bn	–6.6 to –6.2	Vivallo and Henríquez (1998)
	Línce–Estefanía	Cct	–5.7 to –3.0	Vivallo and Henriquez (1998)
		Cct–Dg(–Bn)	–5.2 to + 2.1	Sasaki et al. (1984); Munizaga and Zentilli (1994); Vivallo and Henríquez (1998); Tristá-Aguilera et al. (2006)
	Buena Vista	Cct–Dg	–3.8 to –3.1	Kojima et al. (2009)
	Mantos Blancos	Cct–Dg	–3.2 to –0.1	Sasaki et al. (1984); Munizaga and Zentilli (1994); Ramírez et al. (2006)
		Ccp–Py	–4.5 to + 1.2	Sasaki et al. (1984); Ramírez et al. (2006)
	Santo Domingo	Bn	–2.3	Vivallo and Henríquez (1998)
Cretaceous Belt	Ocoita-Pabellón	Bn–Ccp–Ttr	–44.7 to –25.4	Cisternas and Hermosilla (2006)
		Cct–Cv	–21.9 to –17.9	Cisternas and Hermosilla (2006)
	Talcuna	Cct–Bn–Ccp	–38.3 to –16.0	Spiro and Puig (1988); Carrillo-Rosúa et al. (2006)
	Cerro Negro	Bn	–21.2 to –15.7	Munizaga et al. (1994)
		Ccp	–21.2 to –15.6	Munizaga et al. (1994)
	El Soldado	Cct	–12.7 to –4.6	Villalobos (1995); Wilson et al. (2003b)
		Cct–Bn	–2.2 to + 15.2	Villalobos (1995); Wilson et al. (2003b)
		Bn	–6.9 to + 10.5	Klohn et al. (1990); Wilson et al. (2003b)
		Bn–Ccp	–4.1 to + 19.0	Klohn et al. (1990); Wilson et al. (2003b)
		Ccp	–6.8 to + 7.7	Klohn et al. (1990); Villalobos (1995); Wilson et al. (2003b)
	Lo Aguirre	Bn–Cct–Ccp–Py	–3.6 to + 1.4	Spiro and Puig (1988); Saric et al. (2003)
	Melipilla-Naltahua	Bn	–49.1 to –2.8	Carrillo-Rosúa et al. (2014)
		Bn–Dj	–50.4 to –4.7	Carrillo-Rosúa et al. (2014)
		Ccp	–37.1 to –0.6	Carrillo-Rosúa et al. (2014)
	La Serena area	Bn	–31.7 to –18.9	Carrillo-Rosúa et al. (2014)
		Bn–Dj	–35.0 to –15.5	Carrillo-Rosúa et al. (2014)
		Ccp	–30.8 to –16.8	Carrillo-Rosúa et al. (2014)

Bn, bornite; *Ccp*, chalcopyrite; *Cct*, chalcocite; *Cv*, covellite; *Dg*, "chalcocite"; *Dj*, djurleite; *Py*, pyrite; *Ttr*, tetrahedrite

Constraints on the formation of stratabound Cu–(Ag) deposits

Two hypotheses have been proposed to explain the formation of stratabound Cu–(Ag) deposits in northern Chile: a syngenetic and an epigenetic model (Sato 1984; Vivallo and Henríquez 1998; Kojima et al. 2003, 2009). Geological evidence supports an epigenetic model including the geometry and spatial distribution of the ore bodies mostly related to fault zones and/or intrusive dikes, and the ubiquitous metamorphic/hydrothermal alteration (albitization, chloritization and sericitization) associated with the ore bodies within the volcanic host rocks (Palacios and Definis 1981; Espinoza et al. 1996; Maksaev and Zentilli 2002). Although the epigenetic/hydrothermal origin of these ore deposits is the most accepted hypothesis (Chavez 1985; Palacios 1990; Espinoza et al. 1996; Maksaev and Zentilli 2002; Kojima et al. 2009), there is no consensus on the origin of the ore-forming fluids and the source of metals and ligands such as copper and sulfur, respectively. Two main ideas have been proposed for the origin of the sulfur and metals: i) derived from cooling intrusions (e.g., Palacios 1990; Vivallo and Henriquez 1998) and ii) derived from sedimentary units and/or by leaching of the volcanic host rocks (Losert 1973; Sato 1984; Tosdal and Munizaga 2003; Kojima et al. 2009).

The magmatic-hydrothermal model is based on the close spatial association between the ore bodies and gabbroic to dioritic dike intrusions (Palacios 1990; Espinoza et al. 1996; Vivallo and Henríquez 1998). However, most of the subvolcanic intrusive bodies are usually barren or poorly mineralized (Maksaev and Zentilli 2002). Isotopic data (Sr, Pb, and Os isotopes) are consistent with a strong crustal component in the formation of these deposits (Maksaev and Zentilli 2002; Tosdal and Munizaga 2003; Tristá-Aguilera et al. 2006; Kojima et al. 2003, 2009). On the other hand, stable isotope studies show that in Jurassic deposits the sulfur was derived from a magmatic source, either from the cooling magmas or from leaching of volcanic host rocks, whereas in Cretaceous deposits, sulfides display a wide range of $\delta^{34}S$ with distinct negative values indicating a significant biogenic contribution. The latter is further supported by the presence of framboidal pyrite and, in some cases, bitumen. Regardless of this significant biogenic sulfur source, small to moderate magmatic contributions cannot be ruled out.

The host rock leaching model proposes that hydrothermal fluids of magmatic or non-magmatic origin, i.e., metamorphic, basin-related, meteoric, or marine, leached the volcanic and sedimentary rocks and therefore extract Cu and sulfur. In this model, hydrothermal fluid circulation is supported by the heat of cooling deep plutons and/or dikes (Tosdal and Munizaga 2003; Kojima et al. 2003, 2009). The leaching of copper from source rocks has been attributed to the ability of low-temperature, interstitial, chloride-rich brines to dissolve important amounts of Cu under oxidizing, near-neutral pH conditions (Brown 1971, 2005, 2009; Rose 1976, 1989).

The host-rock leaching hypothesis is tested here by a simple mass balance calculation of the volume of leached volcanic rock and hydrothermal fluid required to produce an average stratabound Cu–(Ag) deposit using the approach of Hofstra and Cline (2000) for Carlin-type deposits. Reported copper resources for Las Luces are 2.3 Mt at 1.11% Cu, which corresponds to a total of ~ 26,000 tons of Cu. Considering a fluid with 50 ppm Cu and assuming that 100% of the dissolved copper precipitates—a valid assumption considering that changes in the Cu solubility due to cooling and/or dilution would yield a high precipitation efficiency—a total volume of fluid required is ~ 0.6 km^3. This can be graphically represented as a cube of 0.8-km side. The average copper content of the La Negra Formation is 100 ppm (Oliveros et al. 2007; Maureira 2018), considering a 50% leaching efficiency, the hydrothermal fluid can scavenge 50 ppm of Cu from the host rock, representing a rock (andesite) volume of 0.2 km^3, corresponding to a water/rock (w/r) ratio of 2.89.

Similarly, the reported copper resources from the Altamira deposit are 2.7 Mt at 1.24% Cu, which represents a total of 33,480 tons of Cu. Assuming a hydrothermal fluid with 40 ppm Cu and a 100% precipitation efficiency, it implies leaching a volume of rock of ~ 0.33 km^3 and a w/r ratio of ~ 2.7 (see details in the Supplemental Material file). The average copper content of the Aeropuerto Formation is 40 ppm (Maureira 2018), and hence, our calculation assumes a very high leaching efficiency (100%), which is very unlikely to occur but provides minimum constraints on the volume of leached rock and the w/r ratios, i.e., extent of hydrothermal alteration. The high w/r ratios calculated by the simple mass balance for both deposits, contrast with the very low w/r ratio estimated for metamorphic ore deposits, which usually have low water/rock ratios (one or two orders of magnitude lower). In the Altamira and Las Luces deposits, the high w/r ratios indicate a process of hydrothermal fluid circulation along fault-fracture networks for the formation of the Cu mineralization, where the stocks and dikes that intruded the host rocks could provide the energy for the circulation of non-magmatic fluids (seawater/basinal brines, connate, and meteoric waters) which leached the metals from the source rocks.

We have mentioned that, in some cases, a significant portion of sulfur required to form the Cu–(Fe) sulfides is sourced from the (sedimentary) host rocks as evidenced by sulfur isotope data. It follows that at least part of the Cu could also be derived from the host rocks; however, the mineralogical form of Cu in the host rocks has not been investigated. One plausible explanation is that Cu is present as magmatic sulfide globules or inclusions within silicate phases such as plagioclase (Keith et al. 1997; Halter et al. 2002). The studied deposits show evidence of pervasive Na alteration of plagioclase phenocrysts in the host rocks (Figs. 4 and 6), providing support for the leaching hypothesis. However, the very high leaching efficiency (~ 80–100%) required to form these Cu deposits is not consistent with a model where the host rock is the sole

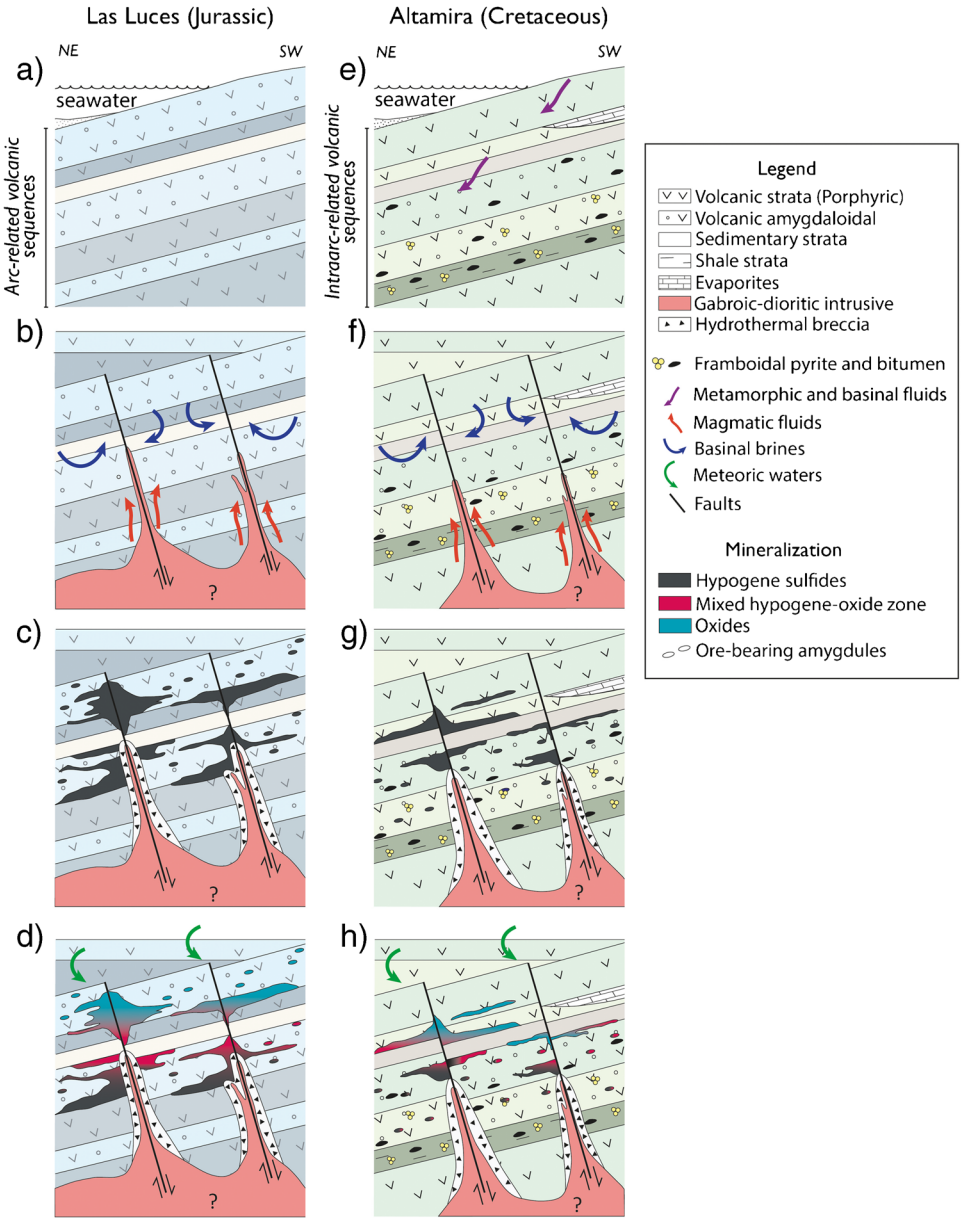

Fig. 14 Schematic model for the formation of Chilean Cu–(Ag) stratabound deposits. **a** and **e** Deposition of volcanic and/or volcanoclastic strata. In intra-arc sequences and during diagenesis, framboidal pyrite and bitumen are formed; minor sulfides (pyrite + chalcopyrite) might also be precipitated. **b** and **f** Hypogene stage begins with the intrusion of gabbroic–dioritic dikes producing heat and convection of the trapped basinal brines or connates waters, which leach host rock, extracting metals (Cu and Ag) and S. **c** and **g** Precipitation of Cu–(Fe) sulfides along faults and within permeable strata, forming hydrothermal breccias in the former and ore "mantos" in the host rocks. **d** and **h** During the Late Cretaceous, basin inversion causes uplift, exposing the ore bodies to more oxidizing conditions and hence, supergene alteration. See text for discussion

source of metals, but it certainly supports that at least a fraction of Cu (and sulfur) is derived from the wall rocks.

Overall, the new data presented here coupled with previous work on the Chilean stratabound Cu–(Ag) deposits show that these ore deposits are likely the result of hydrothermal fluids of mixed origin (basinal brines, meteoric, and magmatic fluids) that circulate through and leached metals and sulfur contained in volcanic or volcano-sedimentary sequences (Fig. 14). Fluid circulation is favored through faults, and metal precipitation occurs along structures and in permeable host rock strata due to fluid cooling, mixing/dilution with meteoric waters, and/or by redox reactions with organic matter (bitumen) or early framboidal pyrite (Maksaev and Zentilli 2002; Kojima et al. 2009; Herazo et al. 2020, 2021).

Conclusions

The Las Luces and the Altamira stratabound Cu–(Ag) deposits are spatially and genetically associated with the Atacama Fault Zone in the Coastal Cordillera of northern Chile. Both deposits are located at about 25°45″S, with Altamira situated ~ 65 km east of Las Luces (Fig. 2); however, Las Luces is hosted by Jurassic volcanic rocks of the La Negra Formation, whereas the Altamira deposit is in Early Cretaceous volcano-sedimentary sequences of the Aeropuerto Formation. Both formations have similar geochemical characteristics, but were emplaced under different tectonic settings; i.e., in an extensional, intra-arc domain (Las Luces), and in an intra-arc basin environment (Altamira).

Both deposits are characterized by sodic–calcic alteration and a mineralization assemblage dominated by Cu sulfides ("chalcocite" group) with variable amounts of bornite, and minor pyrite and chalcopyrite. Framboidal pyrite, possibly formed during diagenesis (Vallentyne 1963; Schallreuter 1984; Oenema 1990; Wilkin and Barnes 1997), was observed in Altamira, but bitumen, a common phase in Cretaceous manto deposits in central Chile, was not found. The chalcocite series minerals as determined in this study support low formation temperatures (< 300 °C) for this deposit type, possibly as low as ~ 100 °C.

In Las Luces, Ag is present in both "chalcocite" (mean 0.08 wt%) and bornite (mean 0.13 wt%), whereas in Altamira bornite is scarce and Ag values in "chalcocite" are similar to those reported for Las Luces bornite and "chalcocite" (mean 0.15 wt%). Silver is preferentially incorporated in solid solution in sulfides, although we cannot rule out the presence of "invisible" Ag-bearing nanoinclusions as reported in other stratabound Cu–(Ag) deposits (Reich et al. 2010, 2013) or Ag-bearing sulfide minerals and microparticles formed outside of sulfide phases like those observed in Altamira (Maureira 2018).

The Las Luces sulfur isotope data (δ^{34}S: –2.5 to + 2.9‰) indicate a magmatic source for the sulfur, whereas in Altamira the extremely negative values (δ^{34}S: –38.7 to –10.7‰) are consistent with sulfur derived by bacterial reduction of marine sulfate as seen in several Cretaceous manto deposits.

Regarding the source of Cu, mass balance calculations show that at least some of the Cu could have been derived from leaching of the host rocks; however, it is unlikely that the wall rocks are the sole source of metals for the formation of these manto-type deposits. Overall, the geological, mineralogical, and analytical data indicate that stratabound Cu–(Ag) deposits are formed by a confluence of different factors and variable contributions of magmatic and non-magmatic sources. Fluids of either magmatic or non-magmatic (basinal brines, connate, meteoric waters) or a combination of both transport metals (Cu, Fe, Ag) and ligands of magmatic origin and/or extracted from the host rocks. These fluids circulated through faults and fractures reaching permeable strata and precipitated their metal content because of cooling or mixing with oxidized (meteoric?) fluids.

Supplementary Information The online version contains supplementary material available at https://doi.org/10.1007/s00126-022-01132-0.

Acknowledgements We acknowledge additional support by ANID through Millennium Science Initiative Program (NCN13_065) "Millennium Nucleus for Metal Tracing Along Subduction." We thank Owen Neill at Washington State University for his support and help with the EPMA analyses. We thank Compañía Minera Las Cenizas S.A. for access to drill cores and mine operations, and mine geologists Carlos García, Jorge Knabe, Diego García, and Víctor Faúndez for discussions regarding the geology of Las Luces and Altamira. We acknowledge Editor Bernd Lehmann, Marcos Zentilli, and an anonymous reviewer for their constructive and helpful comments.

Author contribution All authors contributed to the study conception and design. Material preparation, data collection, and analysis were performed by Ignacio Maureira. The first draft of the manuscript was written by Ignacio Maureira and Fernando Barra and all authors commented on previous versions of the manuscript. All authors read and approved the final manuscript.

Funding This study was funded by ANID-FONDECYT grant #1140780 and #1190105 to F. Barra and M. Reich.

Declarations

Conflict of interest The authors declare no competing interests.

References

Arabasz WJ (1968) Geologic structure of the Taltal area, Northern Chile, in relation to the earthquake of December 28, 1966. Bull Seismol Soc Am 58:835–842

Barra F, Reich M, Selby D, Rojas P, Simon A, Salazar E, Palma G (2017) Unraveling the origin of the Andean IOCG clan: a Re-Os isotope approach. Ore Geol Rev 81:62–78

Boric R, Díaz F, Maksaev V (1990) Geología y yacimientos metalíferos de la Región de Antofagasta. Servicio Nacional de Geología y Minería, Boletín No 40, p 246

Boric R, Holmgren C, Wilson NSF, Zentilli M (2002) The geology of the El Soldado manto type Cu (Ag) deposit, Central Chile. In: Porter TM (ed), Hydrothermal iron oxide copper-gold & related deposits. A global perspective. PGC Publishing, Adelaide 2:163–184

Brown AC (1971) Zoning in the White Pine copper deposit, Ontonogan County, Michigan. Econ Geol 66:543–573

Brown AC (2005) Refinements for footwall red-bed diagenesis in the sediment-hosted stratiform copper deposits model. Econ Geol 100:765–771

Brown AC (2009) A process-based approach to estimating the copper derived from red beds in the sediment-hosted stratiform copper deposit model. Econ Geol 104:857–868

Brown M, Diaz F, Grocott J (1993) Displacement history of the Atacama fault system 25°00′ S-27°00′ S, northern Chile. Geol Soc Am Bull 105:1165–1174

Camus F (1990) The geology of hydrothermal gold deposits in Chile. J Geochem Explor 36:197–232

Carrillo-Rosúa FJ, Morales-Ruano S, Morata D, Boyce AJ, Fallick AE, Belmar M, Munizaga F, Fenoll Hach-Alí P (2006) Mineralogía e isótopos estables en depósitos de Cu (Ag) estratoligados tipo manto del cretácico inferior de la cordillera de la costa (área de La Serena y Melipilla). Actas XI Congreso Geológico Chileno, Antofagasta 2:199–202

Carrillo-Rosúa J, Boyce AJ, Morales-Ruano S, Morata D, Roberts S, Munizaga F, Moreno-Rodríguez V (2014) Extremely negative and inhomogeneous sulfur isotope signatures in Cretaceous Chilean manto-type Cu–(Ag) deposits, Coastal Range of central Chile. Ore Geol Rev 56:13–24

Cembrano J, González G, Arancibia G, Ahumada I, Olivares V, Herrera V (2005) Fault zone development and strain partitioning in an extensional strike-slip duplex: A case study from the Mesozoic Atacama fault system, Northern Chile. Tectonophysics 400:105–125

Chávez W (1985) Geological setting and the nature and distribution of disseminated copper mineralization of the Mantos district, Antofagasta Province, Chile. Unpublished PhD dissertation, California University, Berkeley, USA, p 142

Cioacă ME, Munteanu M, Qi L, Costin G (2014) Trace element concentrations in porphyry copper deposits from Metaliferi Mountains, Romania: a reconnaissance study. Ore Geol Rev 63:22–39

Cisternas ME, Hermosilla J (2006) The role of bitumen in stratabound copper deposit formation in the Copiapo area, Northern Chile. Miner Deposita 41:339–355

Coleman ML, Moore MP (1978) Direct reduction of sulfates to sulfate dioxide for isotopic analysis. Anal Chem 50:1594–1595
Cook NJ, Ciobanu CL, Danyushevsky LV, Gilbert S (2011) Minor and trace elements in bornite and associated Cu–(Fe)-sulfides: A LA-ICP-MS study. Geochim Cosmochim Acta 75:6473–6496
Crespo J, Reich M, Barra F, Verdugo JJ, Martínez C (2018) Critical metal particles in copper sulfides from the supergiant Río Blanco porphyry Cu–Mo deposit Chile. Minerals 8:519
Crespo J, Reich M, Barra F, Verdugo JJ, Martínez C, Leisen M, Romero R, Morata D, Marquardt C (2020) Occurrence and distribution of silver in the world-class Río Blanco porphyry Cu-Mo deposit, Central Chile. Econ Geol 115:1619–1644
Elgueta S, Hodgkin A, Rodriguez E, Schneider A (1990) The Cerro Negro mine, Chile: Manto-type copper mineralization in a volcaniclastic environment. In: Fontboté L, Amstutz GC, Cardozo M, Cedillo E, Frutos J (eds) Stratabound ore deposits in the Andes. Society for Geology Applied to Mineral Deposits, Spec Publ 8, Springer, Berlin, Heidelberg, pp 463–471
Espinoza S, Véliz H, Esquivel J, Arias J, Moraga A (1996) The cupriferous province of the Coastal Range, northern Chile. In: Camus F, Sillitoe RH, Petersen R (eds) Andean copper deposits: new discoveries, mineralization, styles and metallogeny. SEG Spec Pub 5:19–32
Fleet ME (2006) Phase equilibria at high temperatures. Rev Mineral Geochem 61:365–419
González L, Dunai T, Carrizo D, Allmendinger R (2006) Young displacements on the Atacama Fault System, northern Chile from field observations and cosmogenic ^{21}Ne concentrations. Tectonics 25:TC3006 https://doi.org/10.1029/2005TC001846
Grguric BA, Putnis A (1999) Rapid exsolution behaviour in the bornite–digenite series, and implications for natural ore assemblages. Mineral Mag 63:1–12
Grguric BA, Harrison RJ, Putnis A (2000) A revised phase diagram for the bornite-digenite join from in situ neutron diffraction and DSC experiments. Mineral Mag 64:213–231
Halter WE, Pettke T, Heinrich CA (2002) The origin of Cu/Au ratios in porphyry-type ore deposits. Science 296:1844–1846
Herazo A, Reich M, Barra F, Morata D, del Real I, Pagès A (2020) Assessing the role of bitumen in the formation of stratabound Cu-(Ag) deposits: insights from the Lorena deposit, Las Luces district, northern Chile. Ore Geol Rev 124:103639
Herazo A, Reich M, Barra F, Morata D, del Real I (2021) Trace element geochemistry of pyrite from bitumen-bearing stratabound Cu–(Ag) deposits, Northern Chile. ACS Earth Space Chem 5:566–579
Hervé M (1987) Movimiento normal de la Falla Paposo, zona de Falla Atacama, en el Mioceno, Chile. Andean Geology 31:31–36
Hofstra AH, Cline JS (2000) Characteristics and models for carlin-type gold deposits. In: Hagemann SG, Brown PE (eds) Gold in 2000. Rev in Econ Geol 13:163–220
Jara JJ, Barra F, Reich M, Leisen M, Romero R, Morata D (2021) Episodic construction of the early Andean Cordillera unravelled by zircon petrochronology. Nat Commun 12(1):4930. https://doi.org/10.1038/s41467-021-25232-z
Keith JD, Whitney JA, Hattori K, Ballantyne GH, Christiansen EH, Barr DL, Cannan TM, Hook CJ (1997) The role of magmatic sulfides and mafic alkaline magmas in the Bingham and Tintic mining districts, Utah. J Petrol 38:1679–1690
Klohn E, Holmgren C, Ruge H (1990) El Soldado, a strata-bound copper deposit associated with alkaline volcanism in the central Chilean Coastal Range. In: Fontboté L, Amstutz GC, Cardozo M, Cedillo E, Frutos J (eds) Stratabound ore deposits in the Andes. Society for Geology Applied to Mineral Deposits, Spec Publ 8, Springer, Berlin, Heidelberg, pp 435–448
Kojima S, Astudillo J, Rojo J, Tristá D, Hayashi K (2003) Ore mineralogy, fluid inclusion, and stable isotopic characteristics of stratiform copper deposits in the Coastal Cordillera of Northern Chile. Miner Deposita 38:208–216
Kojima S, Tristá-Aguilera D, Hayashi K (2009) Genetic aspects of the manto-type copper deposits based on geochemical studies of North Chilean deposits. Resour Geol 59:87–98
Liu J, Li W, Zhu X, Zhou JX, Yu H (2020) Ore genesis of the Late Cretaceous Larong porphyry W-Mo deposit, eastern Tibet: evidence from in-situ trace elemental and S-Pb isotopic compositions. J Asian Earth Sci 190:104199
Losert J (1973) Genesis of copper mineralization and associated alterations in the Jurassic volcanics rocks of Buena Esperanza mining area. Publicación N°40, Departamento de Geología, Universidad de Chile, Santiago, p 104
Maksaev V (1990) Metallogeny, geological evolution, and thermochronology of the Chilean Andes between latitudes 21° and 26° south, and the origin of major porphyry copper deposits. Unpublished PhD dissertation, Dalhousie University, Halifax, Canada, p 554
Maksaev V, Zentilli M (2002) Chilean strata-bound Cu-(Ag) deposits: an overview. In: Porter TM (ed), Hydrothermal iron oxide copper-gold & related deposits. A global perspective. PGC Publishing, Adelaide 2:185–205
Maureira I (2018) A comparative study between Altamira and las Luces deposits, coastal range, Antofagasta region: implications for the origin of the stratabound Cu–(Ag) deposits. MSc thesis, Universidad de Chile, Santiago, Chile, p 225
Mitchell TM, Faulkner DR (2009) The nature and origin of off-fault damage surrounding strike-slip fault zones with a wide range of displacements: a field study from the Atacama fault system, northern Chile. J Struct Geol 31:802–816
Morales S, Belmar M, Morata D, Carrillo J, Hasler K, Aguirre L, Fenoll P (2005) Relationships between very low-grade metamorphism and Cu-stratabound ore deposits in the Coastal Range of Central Chile. 6th International Symposium on Andean Geodynamics (ISAG 2005, Barcelona). Extended Abstracts 1:527–530
Morata D, Féraud G, Schärer U, Aguirre L, Belmar M, Cosca M (2006) A new geochronological framework for Lower Cretaceous magmatism in the Coastal Range of central Chile. Actas XI Congreso Geológico Chileno 2:509–512
Morata D, Féraud G, Aguirre L, Arancibia, G, Belmar M., Morales S, Carrillo J (2008) Geochronology of the Lower Cretaceous volcanism from the Coastal Range (29°20′–30°S), Chile. Rev Geol Chile 35:123–145
Moreno-Rodríguez V, Carrillo-Rosúa J, Morales-Ruano S, Ruiz-Cárdenas M, Figueroa-Cisterna J, Río Salas R, Chesley J, Ruiz J (2010) Origen de los metales en depósitos tipo "manto" y skarn. Isótopos de Pb y Cu (Cabildo, Chile Central). Macla 13:161–162
Mpodozis C, Ramos V (1990) The Andes of Chile and Argentina. In: Ericksen E, Cañas Pinochet T, Reinemund A (eds) Geology of the Andes and its relation to hydrocarbon and mineral resources. Circum-Pacific Council for Energy and Mineral Resources, Earth Science Series 11:59–90
Munizaga F, Zentilli M (1994) Caracterización isotópica del azufre de los depósitos estratoligados de Cu en Chile. Comunicaciones 45:127–134
Munizaga F, Reyes JC, Nystrom JO (1994) Razones isotópicas de S de los sulfuros del distrito minero Cerro Negro: un posible indicador de los depósitos estratoligados de Cu hospedadas en rocas sedimentarias lacustres. Rev Geol Chile 21:189–195
Naranjo J, Puig A (1984) Hojas Taltal y Chañaral, Regiones de Antofagasta y Atacama, escala 1: 250.000, Carta Geológica de Chile Nº 62–63
Oenema O (1990) Pyrite accumulation in salt marshes in the Eastern Scheldt, southwest Netherlands. Biogeochemistry 9:75–98
Oliveros V, Féraud G, Aguirre L, Fornari M (2005) The beginning of the Andean subduction system: ^{40}Ar/^{39}Ar dating of magmatic activity and subsequent very low-grade metamorphism/hydrothermal alteration in a Jurassic volcanic arc, Coastal Range, northern Chile (18°30'-23°30'S, 70°-70°30'W). 6th International Symposium on Andean Geodynamics (ISAG 2005, Barcelona), Extended Abstracts, pp 555–558
Oliveros V, Féraud G, Aguirre L, Fornari M, Morata D (2006) The early Andean magmatic province (EAMP): ^{40}Ar/^{39}Ar dating on

Mesozoic volcanic and plutonic rocks from the Coastal Cordillera, Northern Chile. J Volcanol Geotherm Res 157:311–330
Oliveros V, Tristá-Aguilera D, Féraud G, Morata D, Aguirre L, Kojima S, Ferraris F (2007) Time relationships between volcanism–plutonism–alteration–mineralization in Cu-stratabound ore deposits from the Michilla mining district, northern Chile: a $^{40}Ar/^{39}Ar$ geochronological approach. Miner Deposita 43:61–78
Oliveros V, Féraud G, Aguirre L, Ramírez L, Fornari M, Palacios C, Parada M (2008) Detailed $^{40}Ar/^{39}Ar$ dating of geologic events associated with the Mantos Blancos copper deposit, northern Chile. Miner Deposita 43:281–293
Oyarzún R, Ortega L, Sierra J, Lunar R, Oyarzún J (1998) Cu, Mn, and Ag mineralization in the Quebrada Marquesa quadrangle, Chile: the Talcuna and Arqueros districts. Miner Deposita 33:547–559
Palacios C, Definis A (1981) Geología del yacimiento estratiforme Susana, distrito Michilla, Antofagasta. Primer Coloquio sobre volcanismo y metalogénesis, Departamento de Geociencias, Universidad del Norte, Antofagasta, Chile, p. 82-91
Palacios C (1990) Geology of the Buena Esperanza Copper-Silver Deposit, Northern Chile. In: Fontboté L, Amstutz GC, Cardozo M, Cedillo E, Frutos J (eds) Stratabound ore deposits in the Andes. Society for Geology Applied to Mineral Deposits, Spec Publ 8, Springer, Berlin, Heidelberg, pp 313–318
Pichowiak S, Buchelt M, Damm KW (1990) Magmatic activity and tectonic setting of the early stages of the Andean cycle in northern Chile. Geol Soc Am Spec Papers 241:127–144
Ramírez LE, Palacios C, Townley B, Parada MA, Sial AN, Fernandez-Turiel JL, Gimeno D, Garcia–Valles M, Lehmann B (2006) The Mantos Blancos copper deposit: an upper Jurassic breccia-style hydrothermal system in the Coastal Range of Northern Chile. Miner Deposita 41:246–245
Reich M, Chryssoulis SL, Deditius A, Palacios C, Zúñiga A, Weldt M, Alvear M (2010) "Invisible" silver and gold in supergene digenite ($Cu_{1.8}S$). Geochim Cosmochim Acta 74:6157–6173
Reich M, Palacios C, Barra F, Chryssoulis S (2013) "Invisible" silver in chalcopyrite and bornite from the Mantos Blancos Cu deposit, northern Chile. Eur J Mineral 25:453–460
Rieger A, Schwark L, Cisternas ME, Miller H (2008) Genesis and evolution of bitumen in Lower Cretaceous lavas and implications for strata-bound copper deposits, North Chile. Econ Geol 103:387–404
Rogers G, Hawkesworth CJ (1989) A geochemical traverse across the North Chilean Andes: evidence for crust generation from the mantle wedge. Earth Planet Sci Lett 91:271–285
Rose AW (1976) The effect of cuprous chloride complexes in the origin of red-bed copper and related deposits. Econ Geol 71:1036–1048
Rose AW (1989) Mobility of copper and other heavy metals in sedimentary environments. In: Boyle RW, Brown AC, Jefferson CW, Jowett EC, Kirkham RV (eds) Sediment-Hosted Stratiform Copper Deposits, Geol Assoc Can Spec Paper 36:97–110
Ruíz, C, Aguirre L, Corvalán J, Klohn C, Klohn E, Levi B (1965) Geología y yacimientos metalíferos de Chile. Instituto de Investigaciones Geológicas, Santiago, Chile, p 302
Saric N, Kreft C, Huete C (2003) Geología del yacimiento Lo Aguirre, Chile. Andean Geol 30:317–331
Sasaki A, Ulriksen CE, Sato K, Ishihara S (1984) Sulfur isotope reconnaissance of porphyry copper and manto-type deposits in Chile and Philippines. Bull Geol Surv Japan 35:615–622
Sato T (1984) Manto type copper deposits in Chile - a review. Bull Geol Surv Japan 35:565–582
Schallreuter R (1984) Framboidal pyrite in deep-sea sediments. Init Rep Deep Sea Drilling Proj 75:875–891
Scheuber E, Andriessen P (1990) The kinematic and geodynamic significance of the Atacama fault zone, northern Chile. J Struct Geol 12:243–257
Scheuber E, González G (1999) Tectonics of the Jurassic-Early Cretaceous magmatic arc of the North Chilean Coastal Cordillera (22°-26°S): a story of crustal deformation along a convergent plate boundary. Tectonics 18:895–910
Shannon RD (1976) Revised effective ionic radii and systematic studies of interatomic distances in halides and chalcogenides. Acta Cryst A32:751–767
Sillitoe RH (2003) Iron oxide-copper-gold deposits: an Andean view. Miner Deposita 38:787–812
Spiro B, Puig A (1988) The source of sulphur in polymetallic deposits in the Cretaceous magmatic arc, Chilean Andes. J South Am Earth Sci 1:261–266
St Amand P, Allen CR (1960) Strike-slip faulting in northern Chile. Geol Soc Am Bull 71:1965
Stoll W (1965) Metallogenic provinces of South America. Min Mag 112(22–33):90–99
Sun T, Bao H, Reich M, Hemming SR (2018) More than ten million years of hyper-aridity recorded in the Atacama gravels. Geochim Cosmochim Acta 227:123–132
Tosdal RM, Munizaga F (2003) Lead sources in Mesozoic and Cenozoic Andean ore deposits, north-central Chile (30–34°S). Miner Deposita 38:234–250
Tristá-Aguilera D, Barra F, Ruíz J, Morata D, Talavera-Mendoza O, Kojima S, Ferraris F (2006) Re-Os isotope systematics for the Lince-Estefanía deposit: constraints on the timing and source of copper mineralization in a stratabound copper deposit, Coastal Cordillera of Northern Chile. Miner Deposita 41:99–105
Ulriksen CE (1979) Regional geology, geochronology, and metallogeny of the Coastal Cordillera of Chile between 25°30' and 26° south. MSc thesis, Dalhousie University, Halifax, Canada, p 236
Vallentyne JR (1963) Isolation of pyrite spherules from recent sediments. Limnol Oceanogr 8:16–30
Villalobos HA (1995) Antecedentes para un modelo genético del yacimiento Veta Negra y su relación con el yacimiento de cobre El Soldado. BSc Honours thesis. Universidad de Concepción, Concepción, Chile, 91 p
Vivallo W, Henriquez F (1998) Génesis común de los yacimientos estratoligados y vetiformes de cobre del Jurásico Medio a Superior en la Cordillera de la Costa, Región de Antofagasta, Chile. Andean Geol 25:199–228
Wilkin RT, Barnes HL (1997) Formation processes of framboidal pyrite. Geochim Cosmochim Acta 61:323–339
Will G, Hinze E, Abdelrahman ARM (2002) Crystal structure analysis and refinement of digenite. $Cu_{1.8}S$, in the temperature range 20 to 500ºC under controlled sulfur partial pressure. Eur J Mineral 14:591–598
Wilson NS, Zentilli M (1999) The role of organic matter in the genesis of the El Soldado volcanic-hosted manto-type Cu deposit, Chile. Econ Geol 94:1115–1135
Wilson NS, Zentilli M (2006) Association of pyrobitumen with copper mineralization from the Uchumi and Talcuna districts, central Chile. Int J Coal Geol 65:158–169
Wilson NSF, Zentilli M, Reynolds PH, Boric R (2003a) Age of mineralization by basinal fluids at the El Soldado manto-type copper deposit, Chile: $^{40}Ar/^{39}Ar$ geochronology of K-feldspar. Chem Geol 197:161–176
Wilson NSF, Zentilli M, Spiro B (2003b) A sulfur, carbon, oxygen, and strontium isotope study of the volcanic-hosted El Soldado manto-type copper deposit, Chile: the essential role of bacteria and petroleum. Econ Geol 98:163–174
Zamora A (2011a) Geología Proyecto Las Luces. Internal report
Zamora A (2011b) Geología Proyecto Altamira. Internal report
Zentilli M, Munizaga F, Graves MC, Boric R, Wilson NS, Mukhopadhyay PK, Snowdon LR (1997) Hydrocarbon involvement in the genesis of ore deposits: an example in Cretaceous stratabound (Manto-Type) copper deposits of central Chile. Int Geol Rev 39:1–21